

Aberrant expression and activity of histone deacetylases (HDACs) in lungs of patients with sporadic idiopathic pulmonary fibrosis (IPF)

Martina Korfei^{1,2}; Sylwia Skwarna^{1,2}; Ingrid Henneke^{1,2}; BreAnne MacKenzie^{1,2}; Oleksiy Klymenko^{1,2}; Shigeki Saito³; Clemens Ruppert^{1,2,4}; Daniel von der Beck^{1,2}; Poornima Mahavadi^{1,2}; Walter Klepetko^{5,11}; Saverio Bellusci^{1,2,4}; Bruno Crestani^{6,11}; Soni Savai Pullamsetti^{1,2,7}; Ludger Fink^{2,4,8}; Werner Seeger^{1,2,4}; Oliver Holger Krämer^{9*} and Andreas Guenther^{1,2,4,10,11*#}.

* both authors have contributed equally to the manuscript

#Corresponding Author

Andreas Guenther, M.D.

Department of Internal Medicine II, Justus-Liebig-University Giessen

Klinikstrasse 36, 35392 Giessen Germany

E-mail: Andreas.Guenther@innere.med.uni-giessen.de

Tel.: +49 641 98542502

Fax: +49 641 98542508

Affiliation of co-authors:

¹Department of Internal Medicine, Justus-Liebig-University Giessen, D-35392 Giessen, Germany.

²Universities of Giessen and Marburg Lung Center (UGMLC), Member of the German Center for Lung Research (DZL).

³Department of Medicine, Section of Pulmonary Diseases, Critical Care and Environmental Medicine, Tulane University Health Science Center, New Orleans, LA 70112, USA.

⁴Excellence Cluster Cardio-Pulmonary System (ECCPS), D-35392 Giessen, Germany.

⁵Department of Thoracic Surgery, Vienna General Hospital, A-1090 Vienna, Austria.

⁶CHU Paris Nord-Val de Seine, Hôpital Xavier Bichat-Claude Bernard, F-75018 Paris, France.

⁷Max-Planck-Institute for Heart and Lung Research, Department of Lung Development and Remodeling, D-61231 Bad Nauheim.

⁸Institute of Pathology and Cytology, D-35578 Wetzlar, Germany.

⁹Department of Toxicology, University Medical Center, D-55131 Mainz, Germany.

¹⁰Agaplesion Lung Clinic Waldhof Elgershausen, D-35753 Greifenstein, Germany.

¹¹European IPF Network and European IPF Registry.

Supporting Information: Materials and Methods/Supplementary-Figures

Handling of human lung tissue

Explanted lungs or lobes were obtained from the Dept. of Thoracic Surgery, Vienna (W. Klepetko). Already at the surgical theatre, peripheral lung tissue samples were snap-frozen or placed in 4% (w/v) paraformaldehyde immediately after explantation. Thereafter, the remaining lung lobes were placed on ice, and shipped (together with the other samples) to our institute immediately. Upon arrival, lung lobes were sectioned under the hood on ice according to a predefined algorithm; and additional lung tissue samples from subpleural and hilar regions were placed in 4% (w/v) PFA or snap-frozen in liquid nitrogen. The latter samples were stored at -80°C until used.

Isolation of primary human lung fibroblasts

Primary human lung fibroblast cells were derived from subpleural lung tissue of explanted lungs at the time of transplantation from patients with sporadic IPF (n=8, 44.63 ± 12.14 years; 5 females, 3 males) and non-diseased control-lungs (organ donors, n=4, 46.50 ± 4.80 years; 3 females, one male), or from histologically normal areas of surgical lung specimens from patients undergoing resective surgery for benign or malignant tumors (n=2, 66.00 ± 8.48 years; 2 females).

Primary fibroblastic lines were established by using an outgrowth-technique from explants according to the method by Jordana and coworkers [S1,S2]. In brief, the peripheral lung tissue (size: ~1-2 × 3-4 cm) was washed with RPMI medium; and the pleural margin and vessels were removed from the lung tissue. Thereafter, the lung tissue was chopped/minced into very small pieces (~ 1 mm³), which were placed on a cell culture dish in PBS containing 200 U/mL penicillin and 200 µg/mL streptomycin. Then the pieces were transferred into a 50 mL Falcon-tube and

incubated for 10 min (for further washing) in a volume of 40 mL PBS containing antibiotics at RT, followed by centrifugation (5 min, 248 rcf, RT) and repeated washings in PBS containing antibiotics until the supernatants were clear. After centrifugation, small lung tissue pieces were put into culture medium [MCDB 131 medium (PAN Biotech) containing 10% (v/v) FBS (PAA Laboratories), 100 U/mL penicillin, 100 µg/mL streptomycin, 2 mM L-glutamine (all from Invitrogen), and 2 ng/mL basic-FGF (Invitrogen), 0.5 ng/mL EGF (Sigma) and 5 µg/mL insulin (Invitrogen)] and cultured à 5 mL in four T75 cell culture flasks in a humidified atmosphere of 37°C and 5% CO₂ (with medium change twice weekly). Upon follow up, fibroblastic cells appeared to be growing either out of the tissue pieces or as islets. After 3-4 weeks, the fibroblast layer was nearly confluent (first passage). The small lung tissue pieces were removed, and fibroblastic cells were harvested by trypsinization and centrifugation, and pooled and replated on five T75 cell culture flasks at 37°C and 5% CO₂. After one week, fibroblasts were confluent (passage 2) and harvested resulting in 5 × 2 cell pellets. One cell pellet was replated on a 10 cm tissue culture dish with 10 mL medium (this corresponds to a splitting 1:2), the other nine fibroblast aliquots were frozen and stored in liquid nitrogen. The fibroblasts from a 10 cm-dish could then be split 1:6-1:7 at confluency (passage 3), and fibroblasts were then cultured for phenotyping/biochemical characterization for a time period of four days. Fibroblast aliquots at each passage were frozen and stored in liquid nitrogen.

In general, the purity of isolated IPF-fibroblasts was verified by positive immunostaining for collagen I (mesenchymal marker), and negative staining for MNF-116 (detects an epitope common to many cytokeratins [Moll's numbers 5, 6, 8, 17 and 19]) and vWF (von Willebrand factor, marker for blood vessels). All experiments

were carried out with IPF-fibroblasts and normal fibroblasts between passages 3 and 4.

Cell Culture experiments

Primary fibroblasts of patients with IPF (n=6) were seeded in normal culture medium on 10 cm tissue culture dishes and cultured for 3 days. At 95-99% confluency, IPF-fibroblasts were incubated for 30h with the HDAC inhibitors (HDACi) panobinostat (LBH589, 85nM, from Selleckchem) and valproic acid (VPA, 1.5mM, from Santa Cruz), and as control experiment with the respective solvents (vehicle-control) in the concentration 0.1% (v/v) ethanol and 0.03% (v/v) DMSO.

The pan-HDACi LBH589 has an efficient inhibitory activity at nanomolar concentrations (14-200 nM) and appears to be the most potent clinically available HDAC inhibitor (S3). Valproic acid is a weak class-I-HDACi and efficient in the millimolar range (0.5 – 5.0 mM) (S4,S5). The dosages of HDACi (S3-S5) were chosen according to published - and own preliminary studies. HDACi experiments were performed using culture medium containing 2% (v/v) FBS.

After incubation, fibroblastic cells from each plate were harvested by trypsination and divided in two equal volume parts, and centrifuged using two Falcon-tubes (5 min, 1000 rpm, RT) resulting in two pellets. One pellet was subjected to protein isolation, the other to RNA isolation.

Semiquantitative Reverse Transcription-Polymerase Chain Reaction (RT-PCR)

Total cellular RNA was prepared from treated IPF-fibroblasts using the RNeasy[®] Plus Mini-Kit (Qiagen) and 600 µL RLT Plus-lysis buffer according to the protocol of the manufacturer. The great advantage of the kit is the efficient removal of genomic DNA during the isolation procedure with use of the "gDNA eliminator column". The purity

and quantity of the isolated RNA was determined by spectrophotometry at 260/280 nm using NanoDrop 2000c photometer (PeqLab).

Reverse transcription (RT) and PCR were performed sequentially in two separate steps. Complementary DNA (cDNA, 2 µg) was first synthesized by reverse transcription (RT) using 2 µg total RNA, and with use of oligo-dT-primers and the Omniscript-RT-Kit (Qiagen). An aliquot of the finished RT reaction/cDNA (100 ng) was then used for PCR amplification employing gene-specific primers for transcripts. The complete list of primers used is given in **Table S1**.

Each 40-µL RT reaction contained (final concentration): 2 µg total RNA, 1 µM oligo-dT-primers, 10 units RNase inhibitor (both Applied Biosystems), 500 µM of each dNTP and 4 units Omniscript Reverse Transcriptase (both Qiagen). The RT reactions were incubated for 65 min at 37°C, directly followed by PCR using gene-specific primers. Each 20-µL PCR reaction contained (final concentration): 2 µL finished RT reaction (= 100 ng template cDNA), 0.2 µM each forward and reverse primer (metabion, Martinsried, Germany), 200 µM of each dNTP (Thermo Scientific) and 0.4 µL Phire-Hot-Start-II-DNA-Polymerase (Thermo Scientific), which is a novel PCR enzyme and significantly faster than *Taq*-based polymerases. For amplification of all described mRNA's/genes, a special cycling protocol according to the manufacturer's protocol was performed: "Hot-Start" (initial activation step: 98°C for 30 sec) followed by 3-step-cycling (20-35 cycles of amplification): denaturation: 98°C for 5 s; annealing: 59-65°C for 5 s (the annealing temperatures of each primer pair is given in **Table S1**), extension: 72°C for 15 sec (and 60 sec in the final extension). The thermal cycler used was from Bio-Rad (model: PTC-1148).

As control experiment, PCR reactions of RNA samples without reverse transcriptase were performed (to exclude amplification of genomic DNA contaminations).

Equal aliquots of the PCR products were electrophoresed through a 2% (w/v) agarose gel containing ethidium bromide in 1× tris-acetate-EDTA (TAE) buffer, and documented by scanning using an UV imager (Gel-Doc XR⁺, Bio-Rad). Thereafter, band intensities of PCR products were quantified using Image Lab-Software (version 4.1, Bio-Rad), and mRNA expression of genes of interest were normalized to the expression of *GAPDH*.

Quantitative Real-Time- Polymerase Chain Reaction (qRT-PCR)

For mRNA expression analysis of HDAC6 in IPF- (n=31) and control-lung tissues (n=12), qRT-PCR was performed. RNA was reverse-transcribed using QuantiTect Reverse Transcription Kit (Qiagen). cDNA was diluted to a concentration between 20 ng/μL. Primers were designed using Roche Applied Sciences online Assay Design Tool. All primers were designed to span introns and blasted using NCBI software for specificity. Sybr Green Master Mix (Applied Biosciences) was used for RT-PCR with a Roche LightCycler 480 machine. Samples were run in triplicates using hydroxymethylbilane synthase (*HMBS*) as a reference gene for human samples.

Human Primers	Forward	Reverse
<i>HMBS</i>	5'-AGCTATGAAGGATGGGCAAC-3'	5'-TTGTATGCTATCTGAGCCGTCTA-3'
<i>HDAC6</i>	5'-AACTGAGACCGTGGAGAG-3'	5'-CCTGTGCGAGACTGTAGC-3'

Western Blot analysis

For analysis of HDAC protein expression, peripheral lung tissue samples from the lower lobe, from the subpleural region of the lung was used. Lung homogenates were

prepared of frozen lung tissue samples (size 1 cm³) from IPF patients (n=26) and controls (n=16) according to the protocol previously described [S6].

For preparation of protein extracts from lung fibroblasts, frozen cell pellets were lysed with 100-200 µL cold extraction buffer [50 mmol/L tris-HCl [pH 7.5], 150 mmol/L NaCl, 1% (w/v) triton X-100, 0.5% (w/v) sodium-deoxycholate, 5 mmol/L EDTA, 1 µmol/L trichostatin-A (TSA, Selleckchem), and 1× Halt™ Protease & Phosphatase Cocktail (Thermo Scientific)], and subjected to 3× repeated freezings (in liquid nitrogen) and thawings for efficient cell disruption. Cell lysates were then incubated on ice for 1h, followed by centrifugation (10 min, 13000 rpm, 4°C) to remove cell debris. The resulting supernatants were then stored at -80°C until further use. In general, the protein concentration in lung homogenates and fibroblastic cell extracts was determined according to the Pierce® BCA protein assay from Thermo Scientific.

For one-dimensional SDS-PAGE, lung homogenates or cell lysates were then diluted (1:3) in 4×SDS-sample buffer [leading to a final concentration 2% (w/v) SDS, 2.5% (v/v) β-mercaptoethanol, 10% (v/v) glycerol, 12.5 mmol/L tris-HCl [pH 6.8], 0.1% (w/v) bromophenol blue in samples] and heated for denaturation at 99°C for 15 min. Denaturated proteins from each sample (50 µg/lane in case of lung homogenates, 15 µg/lane in case of fibroblastic cell lysates) were then separated by 8%, 9%, 10%, 12% or 15% Laemmli-SDS-PAGE. Thereafter, the separated proteins were transferred to a PVDF membrane (GE Healthcare) in a semi-dry blotting chamber according to the manufacturer's protocol (Bio-Rad, Munich, Germany). Obtained immunoblots were then blocked by incubating at room temperature for 1 h in blocking buffer [1 × tris-buffered saline (TBS; 50 mmol/L tris-HCl, pH 7.5, 50 mmol/L NaCl) containing 5% (w/v) nonfat dried milk and 0.1 % (w/v) tween 20], followed by immunostaining for proteins of interest. In the following, the primary antibodies used for western blotting are listed, including the sources and dilutions: mouse monoclonal

for HDAC1 (1:500, Abcam, ab46985), rabbit monoclonal for human HDAC2 (1:2000, Abcam, ab32117), rabbit polyclonal for human HDAC3 (1:1000, Santa Cruz B. I., sc-11417), rabbit monoclonal for human HDAC3 (1:2000, Abcam, ab32369), rabbit polyclonal for human HDAC4 (1:500, Santa Cruz B. I., sc-11418), rabbit polyclonal for human HDAC5 (1:500, Abcam, ab55403, non-reducing SDS-PAGE), rabbit polyclonal for human HDAC7 (1:1000, Abcam, ab137366), rabbit polyclonal for human HDAC7 (1:500, Santa Cruz B. I., sc-11421), rabbit polyclonal for human HDAC8 (1:500, Santa Cruz B. I., sc-11405), rabbit polyclonal for human HDAC9/HDRP (1:2000, Abcam, ab59718), rabbit polyclonal for human HDAC9 (1:300, Santa Cruz B. I., sc-28732), rabbit polyclonal for human HDAC10 (1:1000, Abcam, ab53096), sheep polyclonal for human CD90/Thy-1 (1:500, R&D Systems, #AF2067), rabbit polyclonal for human histone H3 [acetyl K27] (1:15000, Abcam, ab4729), rabbit polyclonal for histone H3 (1:10000, Abcam, ab1791), mouse monoclonal for acetylated tubulin [from the outer arm of *Strongylocentrotus purpuratus* (sea urchin)] (1:50000, Sigma, T7451), mouse monoclonal for human p53 (1:250, Santa Cruz B. I., sc-263), mouse monoclonal for human p21 (1:250, Abcam, ab16767), mouse monoclonal for human cyclin D1 (1:250, Abcam, ab10540), rabbit polyclonal for human survivin (1:750, Abcam, ab24479), rabbit polyclonal for human phospho-histone H3 (1:500, Abcam, ab5176), rabbit polyclonal for human Bcl-XL (1:750, Abcam, ab32370), rabbit polyclonal for human CHOP/GADD153 (1:500, Santa Cruz B. I., sc-793), mouse monoclonal for human α -SMA (1:15000, Abcam, ab119952), rabbit polyclonal for collagen α 1-type I [COL1A1] (1:300, Santa Cruz B. I., sc-28657), and rabbit polyclonal for collagen type-I (1:3000, Rockland, #600-401-103). Blots were incubated with primary antibody (diluted in blocking buffer) overnight at 4°C with gentle shaking. The blots were then washed four times in 1 ×

TBS containing 0.1 % (w/v) tween 20, and incubated with respective horseradish peroxidase-conjugated secondary antibodies (DakoCytomation, Hamburg, Germany; rabbit anti-mouse-IgG, rabbit anti-goat-IgG, rabbit anti-sheep IgG, or swine anti-rabbit IgG, all diluted 1:2000 in blocking buffer) for 2 hours at room temperature. After four washes, blot membranes were developed with the Pierce[®] ECL Plus chemiluminescent detection system (Thermo Scientific), and emitted signals were detected with a chemiluminescence imager (Intas ChemoStar, Intas, Göttingen, Germany). Thereafter, blots were stripped using "stripping buffer" [2% (w/v) SDS and 50 mmol/L dithiothreitol in tris-buffered saline (TBS)] under gentle shaking at 70°C for 1h, followed by reprobing the blots using antibodies against the loading control proteins β -actin (ab8226, abcam, diluted 1:3000), GAPDH (sc-20357, Santa Cruz, diluted 1:1000) or tubulin (#T0198, Sigma, diluted 1:2000).

For quantification, band intensities in acquired TIFF/JPEG-images were analyzed by densitometric scanning and quantified using ImageJ software (Version 1.46r, NIH). The band densities were normalized to β -actin, GAPDH or tubulin.

Immunohistochemistry (IHC)

Human lungs were placed in 4% (w/v) paraformaldehyde after explantation (fixation was done for 12 – 24 h), and processed for paraffin embedding. Sections (3 μ m) were cut and mounted on positively charged glass slides (Super Frost Plus, Langenbrinck). Paraffin-embedded tissue sections of normal donor and IPF-lungs were deparaffinized in xylene and rehydrated in graded alcohol. Antigens were retrieved by cooking the sections for 5 min in 10 mmol/L citrate buffer (pH 6.0) using microwave irradiation (800 W). Thereafter, sections had to cool down for 20 min at RT, followed by repeated cookings (800 W, 5 min) and coolings (20 min at RT). This

procedure was performed three times. Importantly, the citrate buffer was freshly prepared by mixing 18 mL 100mmol/L citric acid monohydrate and 82 mL 100mmol/L sodium citrate tribasic dihydrate with 900 mL distilled water.

For immunostaining, the streptavidin-biotin-alkaline phosphatase (AP) - or the streptavidin-biotin- horse radish peroxidase (HRP) method with use of the ZytoChem-Plus AP Kit (Fast Red), Broad Spectrum or the ZytoChem-Plus HRP Kit (DAB-staining, brown dye), Broad Spectrum (Zytomed Systems, Berlin, Germany) according to the manufacturer's protocol were employed.

In the following, the primary antibodies used for IHC are listed, including the sources and dilutions: rabbit polyclonal for human proSP-C (1:750, Millipore, AB3786), rabbit monoclonal for human cytokeratin-5 [KRT5] (1:200, Abcam, ab75869), rabbit polyclonal for human smooth muscle actin [α -SMA] (1:200, Abcam, ab5694), mouse monoclonal for human p63 (1:150, Abcam, ab3239), rat monoclonal for human clara cell-protein 10 [CC10] (1:75, R&D Systems), mouse monoclonal for human FoxJ1/HFH4 (1:75, Abcam), mouse monoclonal for HDAC1 (1:50, Abcam, ab46985), rabbit polyclonal for human HDAC2 (1:50, Santa Cruz Biotechnology Inc., sc-7899), rabbit monoclonal for human HDAC2 (1:200, Abcam, ab32117), rabbit polyclonal for human HDAC3 (1:100, Santa Cruz B. I., sc-11417), rabbit polyclonal for human HDAC4 (1:50, Santa Cruz B. I., sc-11418), rabbit polyclonal for human HDAC5 (1:100, Abcam, ab55403), rabbit monoclonal for human HDAC6 (1:100, Abcam, ab133493), rabbit polyclonal for human HDAC7 (1:100, Abcam, ab137366), rabbit polyclonal for human HDAC8 (1:50, Santa Cruz B. I., sc-11405), rabbit polyclonal for human HDAC9/HDRP (1:100, Abcam, ab59718), rabbit polyclonal for human HDAC10 (1:100, Abcam, ab53096) and rabbit polyclonal for human survivin (1:200, Abcam, ab24479). In general, sections were incubated for 2h with primary antibodies, which were diluted in PBS containing 2% (w/v) BSA.

Detection was performed with a polyvalent secondary biotinylated antibody (rabbit, mouse, rat, guinea pig, provided by the ZytoChem-Plus AP Kit/or ZytoChem-Plus HRP Kit, 20 min incubation) followed by incubation with AP/or HRP conjugated streptavidin (20 min). Sections were then developed with Fast Red/or DAB substrate solution, and the reaction was terminated by washing in distilled water. The stained sections were counterstained with hemalaun (Mayers hemalaun solution, WALDECK Division CHROMA GmbH & CO KG, Münster, Germany) and mounted in Glycergel (DakoCytomation).

Control sections were treated with PBS-2%BSA alone or with rabbit or mouse primary antibody isotype control (#NB810-56910 and #AM03096PU-N, both Acris Antibodies GmbH, Germany) to determine the specificity of the staining.

Lung tissue sections were scanned with a Mirax Desk slide scanning device (Mirax Desk, Zeiss, Germany), and examined histopathologically at 100×, 200×, 400× and 800× original magnification. IHC for mentioned antibodies was undertaken in 10 IPF- and 5 control-lung samples.

Statistics

For the statistical comparison of differences between two groups (IPF vs. control), the Mann Whitney-test was applied. For the statistical comparison of differences between three groups (LBH589-treatment vs. vehicle-treatment, VPA-treatment vs. vehicle-treatment, VPA-treatment vs. LBH589-treatment) the Kruskal-Wallis test with the Dunn's multiple comparison test as post-test was applied. For statistics, the software GraphPad Prism version 5.02 was employed. A p-value < 0.05 was considered statistically significant.

Supplementary References

- [S1] Jordana M, Newhouse MT, Gauldie J. Alveolar macrophage/peripheral blood monocyte-derived factors modulate proliferation of primary lines of human lung fibroblasts. *J Leukoc Biol* 1987;42:51-60.
- [S2] Jordana M, Befus AD, Newhouse MT, et al. Effect of histamine on proliferation of normal human adult lung fibroblasts. *Thorax* 1988;43:552-558.
- [S3] Anne M, Sammartino D, Barginear MF, et al. Profile of panobinostat and its potential for treatment in solid tumors: An update. *Onco Targets Ther* 2013;6:1613-1624.
- [S4] Xu WS, Parmigiani RB, Marks PA. Histone deacetylase inhibitors: Molecular mechanisms of action. *Oncogene* 2007;26:5541-5552.
- [S5] Kramer OH, Zhu P, Ostendorff HP, et al. The histone deacetylase inhibitor valproic acid selectively induces proteasomal degradation of HDAC2. *EMBO J* 2003;22:3411-3420.
- [S6] Korfei M, Schmitt S, Ruppert C, et al. Comparative proteomic analysis of lung tissue from patients with idiopathic pulmonary fibrosis (IPF) and lung transplant donor lungs. *J Proteome Res* 2011;10:2185-2205.

Table E1: Primers used in semiquantitative RT-PCR (homo sapiens)

Gene/Name of primer	Primer-Sequence	Annealing Temp.(T _A)	Size of PCR product	No. of Cycles
<i>HDAC1 forward</i>	5'- GCC GCA AGA ACT CTT CCA AC - 3'	63°C	140 bp	28
<i>HDAC1 reverse</i>	5'- CTT GAC CCC TTT GGC TTC TG - 3'			
<i>HDAC2 forward</i>	5'- CAG GAG ACT TGA GGG ATA TTG G - 3'	65°C	320 bp	25
<i>HDAC2 reverse</i>	5'- ATG TGT CCA ACA TCG AGC AAC - 3'			
<i>HDAC3 forward</i>	5'- CCG GTT ATC AAC CAG GTA GTG - 3'	64°C	321 bp	25-26
<i>HDAC3 reverse</i>	5'- GGT GCT GAC ATC TGG ATG AAG - 3'			
<i>HDAC4 forward</i>	5'- CTT CTG CAG CAG AGG TTG AG - 3'	63°C	267 bp	28
<i>HDAC4 reverse</i>	5'- TCT GAA GGC CGC CAA GTA C - 3'			
<i>HDAC5 forward</i>	5'- TCA ACC GGC AGA AGC TAG AC - 3'	63°C	319 bp	28
<i>HDAC5 reverse</i>	5'- TTG CCC ACG TTC AAC TTC TG - 3'			
<i>HDAC6 forward</i>	5'- CCC AGC ACA GTC TTA TGG - 3'	63°C	320 bp	29
<i>HDAC6 reverse</i>	5'- AGG AAA GCA GCA ATG TAG - 3'			
<i>HDAC7 forward</i>	5'- CTC AAA CTG GAC AAC GGG AAG - 3'	63°C	270 bp	27
<i>HDAC7 reverse</i>	5'- GGC CAC TGA GTT GAA GAA GC - 3'			
<i>HDAC8 forward</i>	5'- GTC CCG AGT ATG TCA GTA TGT G - 3'	65°C	222 bp	27
<i>HDAC8 reverse</i>	5'- CTA TGG AGT CCG GAT GAT CAT C - 3'			
<i>HDAC9 forward</i>	5'- GAA AGG GCA GTG GCA AGT AC - 3'	63°C	222 bp	30
<i>HDAC9 reverse</i>	5'- ATC TTG TGC TCC TGG TAA TGT G - 3'			
<i>HDAC10 forward</i>	5'- GCA GGT GAA CAG TGG TAT AGC - 3'	63°C	220 bp	28
<i>HDAC10 reverse</i>	5'- CGT GGA GAC ATG GAA CAT GG - 3'			
<i>HDAC11 forward</i>	5'- AGG GCT ACC ATC ATT GAT CTT G - 3'	63°C	222 bp	28
<i>HDAC11 reverse</i>	5'- CTG GAG GGA TTT CTT GAT GTT C - 3'			
<i>SIRT1 forward</i>	5'- CAA GCT CTA GTG ACT GGA CTC - 3'	64°C	321 bp	30
<i>SIRT1 reverse</i>	5'- CAT CCC TTG ACC TGA AGT CAG - 3'			
<i>SIRT2 forward</i>	5'- CGG TAC ATG CAG AGC GAA C - 3'	60°C	221 bp	27
<i>SIRT2 reverse</i>	5'- TGC CCA GGA TAG AGT TCC TTG - 3'			
<i>GAPDH forward</i>	5'- ACC CAG AAG ACT GTG GAT GG - 3'	59°C	320 bp	24
<i>GAPDH reverse</i>	5'- GTG TCG CTG TTG AAG TCA GAG - 3'			
<i>ACTB forward</i>	5'- ACC CTG AAG TAC CCC ATC G - 3'	60°C	220 bp	25
<i>ACTB reverse</i>	5'- CAG CCT GGA TAG CAA CGT AC - 3'			
<i>P53 forward</i>	5'- CCT CAG CAT CTT ATC CGA GTG - 3'	64°C	223 bp	25
<i>P53 reverse</i>	5'- GTA GAT TAC CAC TGG AGT CTT CC - 3'			
<i>CIP1 forward</i>	5'- GAT GGA ACT TCG ACT TTG TCA C - 3'	61°C	220 bp	22
<i>CIP1 reverse</i>	5'- GGC ACA AGG GTA CAA GAC AG - 3'			
<i>PUMA forward</i>	5'- ATG GCG GAC GAC CTC AAC - 3'	58°C	119 bp	28
<i>PUMA reverse</i>	5'- CTG GGT AAG GGC AGG AGT C - 3'			
<i>ACTA2 forward</i>	5'- GAG ATC TCA CTG ACT ACC TCA TG - 3'	60°C	269 bp	26
<i>ACTA2 reverse</i>	5'- AGC AGA CTC CAT CCC GAT G - 3'			
<i>COL1A1 forward</i>	5'- TGC CAC TCT GAC TGG AAG AG - 3'	60°C	320 bp	20
<i>COL1A1 reverse</i>	5'- TTG CAG TGG TAG GTG ATG TTC - 3'			
<i>COL3A1 forward</i>	5'- TTA CAA GGC TTA CCT GGT ACA G - 3'	59°C	269 bp	25
<i>COL3A1 reverse</i>	5'- CCA GGC ATT CCT TGC AGA C - 3'			
<i>FN forward</i>	5'- CAT ACC ACG TAG GAG AAC AGT G - 3'	62°C	221 bp	20
<i>FN reverse</i>	5'- AGG CAT GAA GCA CTC AAT TGG - 3'			
<i>CNN1 forward</i>	5'- GAG TGA AGT ACG CAG AGA AGC - 3'	59°C	269 bp	26
<i>CNN1 reverse</i>	5'- CTC GAA GAT CTG CCG CTT G - 3'			

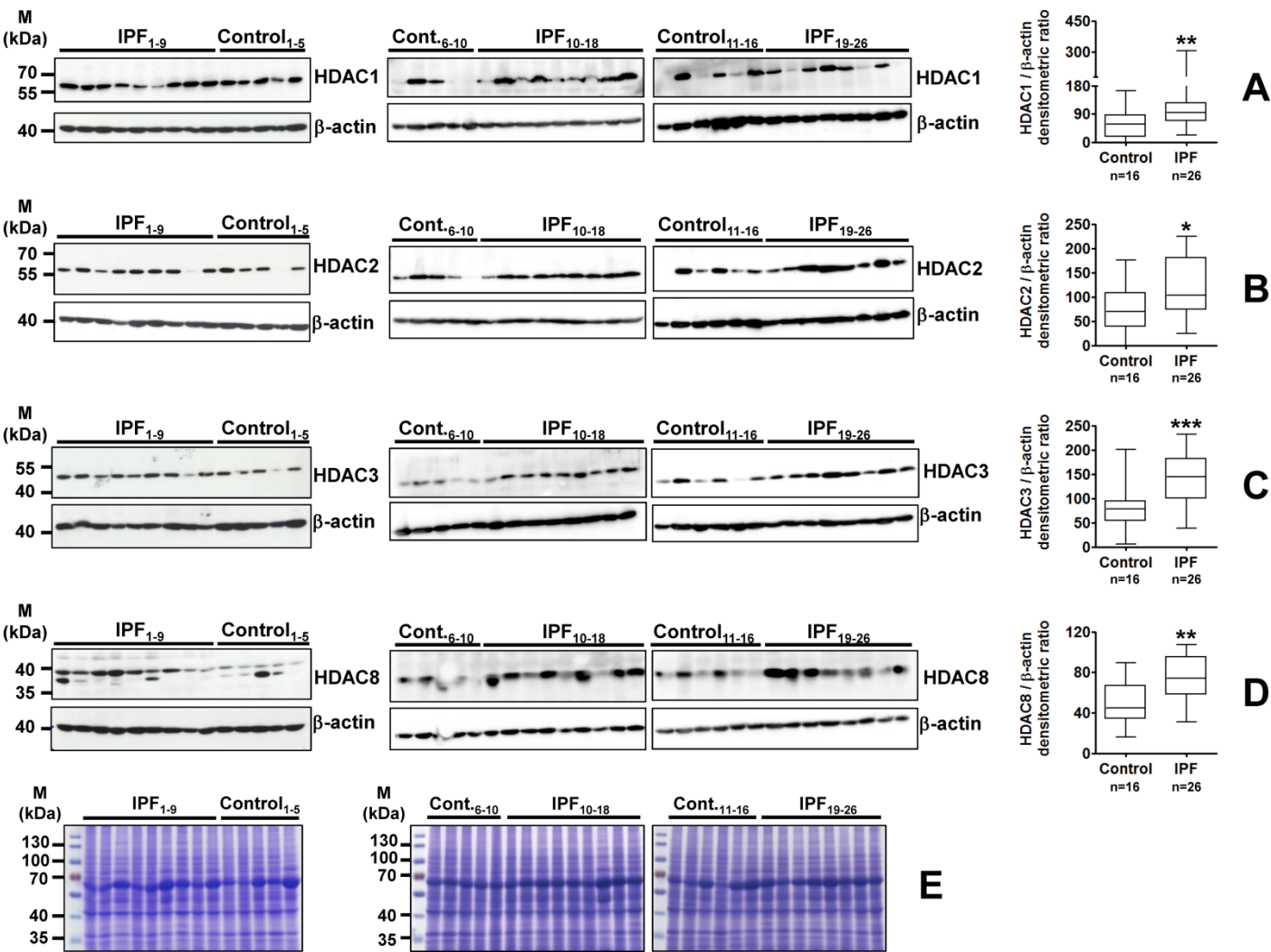
Table E1 continued: Primers used in semiquantitative RT-PCR (homo sapiens)

Gene/Name of primer	Primer-Sequence	Annealing Temp.(T _A) *	Size of PCR product	No. of Cycles
<i>P4HTM forward</i>	5'- TGG ATT ACC TGC CAG AGA GAC - 3'	64°C	272 bp	26
<i>P4HTM reverse</i>	5'- AGT CTC AGG GTC ATG TAC TGT AG - 3'			
<i>VIM forward</i>	5'- AAG CAG GAG TCC ACT GAG TAC -3'	64°C	270 bp	25
<i>VIM reverse</i>	5'- CTT CCT GTA GGT GGC AAT CTC - 3'			
<i>CCND1 forward</i>	5'- CGA GAA GCT GTG CAT CTA CAC - 3'	62°C	221 bp	26
<i>CCND1 reverse</i>	5'- ACT TCA CAT CTG TGG CAC AAG - 3'			
<i>BIRC5 forward</i>	5'- AAA GCA TTC GTC CGG TTG C - 3'	57°C	161 bp	25-26
<i>BIRC5 reverse</i>	5'- GCA CTT TCT TCG CAG TTT CC - 3'			
<i>UBE2L6 forward</i>	5'- CGT TCA AGC CTC CCA TGA TC - 3'	60°C	220 bp	25
<i>UBE2L6 reverse</i>	5'- AGC TCC GGA TTC TGT GTC AG - 3'			
<i>ATF6 forward</i>	5'- ACT CAG GGA GTG AGC TAC AAG - 3'	63°C	270 bp	25
<i>ATF6 reverse</i>	5'- GGA GGA TCC TGG TGT CCA TC - 3'			
<i>CHOP forward</i>	5'- ACT CTC CAG ATT CCA GTC AGA G - 3'	61°C	220 bp	24
<i>CHOP reverse</i>	5'- GCC TCT ACT TCC CTG GTC AG - 3'			

*It has to be noted that the annealing temperature (T_A) for listed primers is only valid for Phire-Hot-Start-II-DNA-Polymerase. The annealing rules for Phire II are different from many common DNA polymerases (such as *Taq* DNA polymerases). As a basic rule, for primers > 20 nt, the T_A is T_m +3°C of the lower T_m primer. For primers ≤ 20 nt, the T_A has to be equal to the T_m of the lower T_m primer.
T_m = melting temperature.

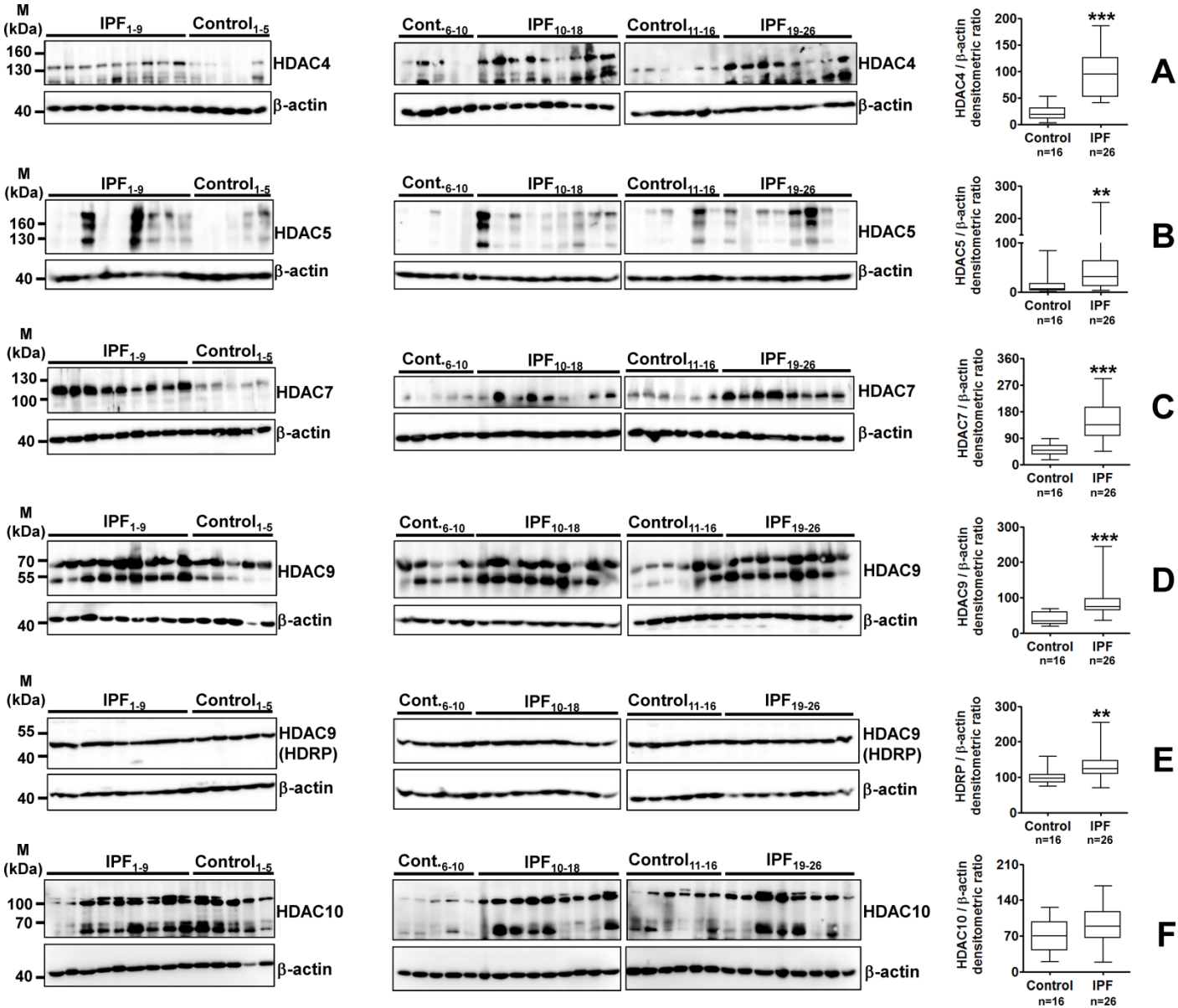
Primers were designed using "GeneFisher/GeneFisher2"-Software - interactive PCR primer design. (<http://bibiserv.techfak.unibielefeld.de/genefisher2/>).
GeneFisher - software support for the detection of postulated genes. *Robert Giegerich, Folker Meyer and Chris Schleiermacher*. Proc Int Conf Intell Syst Mol Biol. 1996;4:68-77.

In the majority, intron-spanning primers were chosen.



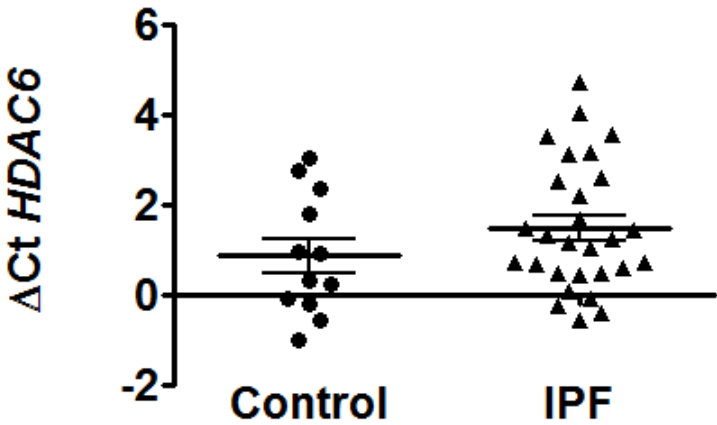
Supplementary-Figure S1: Upregulation of class-I-histone deacetylases in lung tissue from patients with idiopathic pulmonary fibrosis (IPF).

Representative immunoblots (left) and quantitative immunoblot analysis (right) of subpleural lung tissue from patients with sporadic IPF (n=26) and non-diseased control-lungs (control, n=16) using specific antibodies against HDAC1 (**A**), HDAC2 (**B**), HDAC3 (**C**), HDAC8 (**D**), and β -actin as loading control. Representative Coomassie stained gels of 50 μ g proteins extracted from IPF- and control-lungs are shown in (**E**). Densitometric ratios of the respective protein to β -actin are depicted as a box-and whisker diagram (*box* indicates 25th and 75th, *horizontal line* indicates the 50th percentile [median], and extensions above and below reflect extreme values). *p < 0.05, **p < 0.01, ***p < 0.001; by Mann Whitney-test.

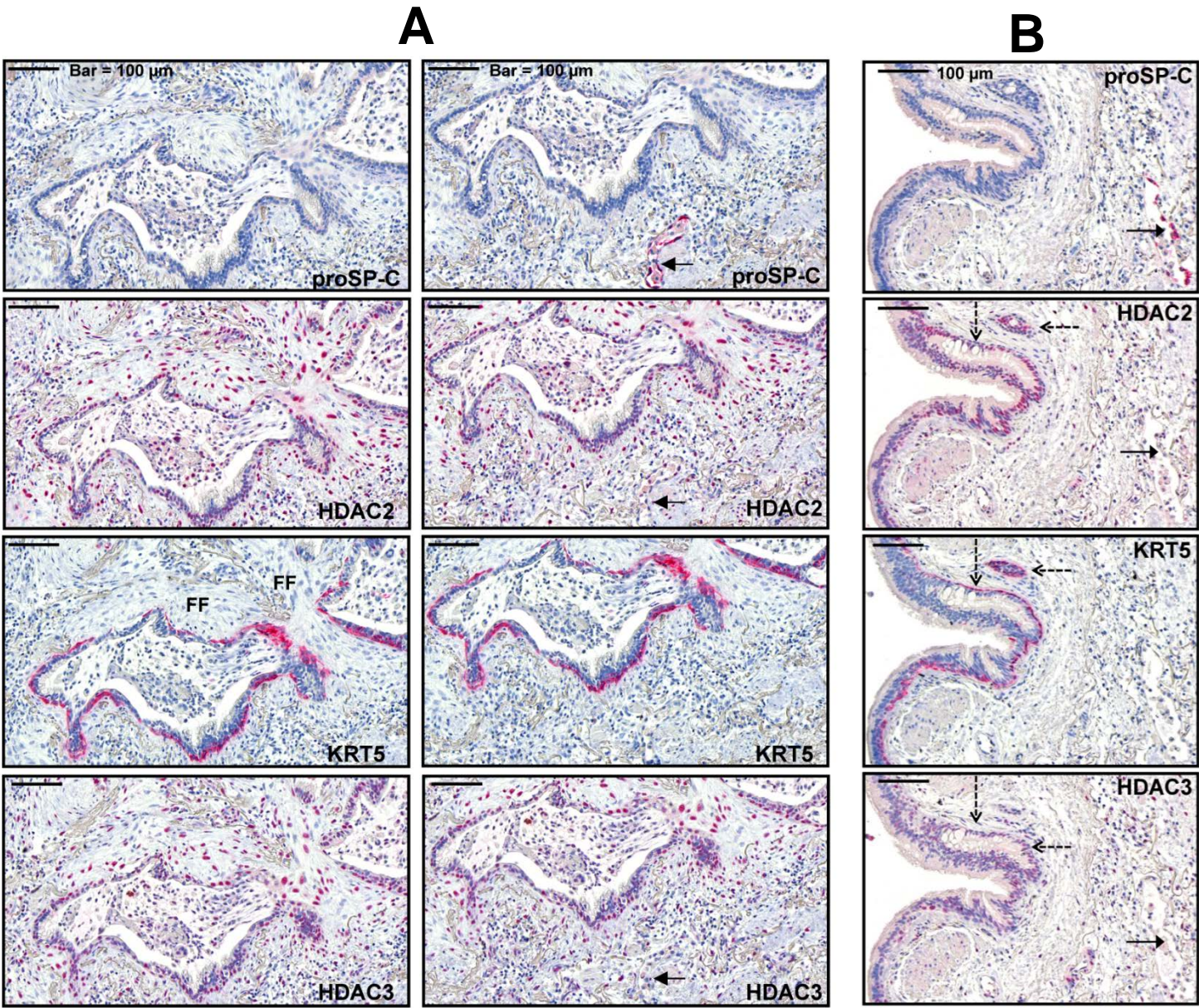


Supplementary-Figure S2: Upregulation of class-II-histone deacetylases in lung tissue from patients with idiopathic pulmonary fibrosis (IPF).

Representative immunoblots (left) and quantitative immunoblot analysis (right) of subpleural lung tissue from patients with sporadic IPF (n=26) and non-diseased control-lungs (control, n=16) using specific antibodies against HDAC4 (A), HDAC5 (B), HDAC7 (C), HDAC9 (D), HDAC9 isoform HDRP (E), HDAC10 (F), and β -actin as loading control. Densitometric ratios of the respective protein to β -actin are depicted as a box- and whisker diagram (box indicates 25th and 75th percentile [median], and extensions above and below reflect extreme values). **p < 0.01, ***p < 0.001; by Mann Whitney-test.



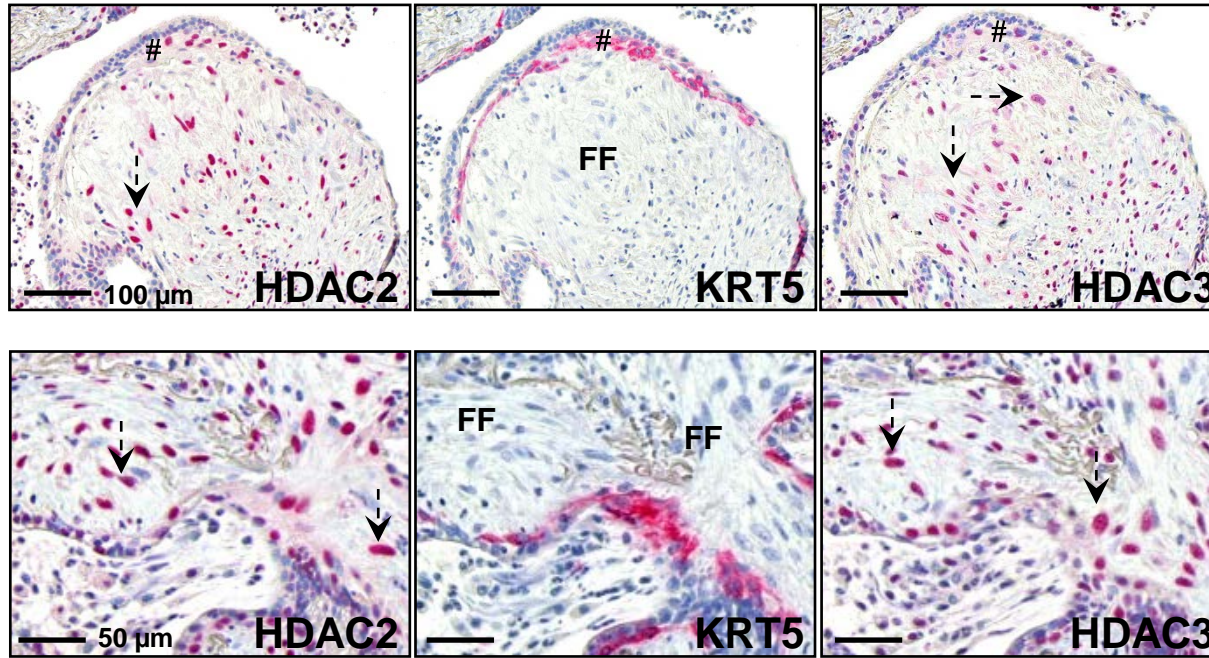
Supplementary-Figure S3: Gene expression analysis for class-IIb-histone deacetylase HDAC6 in control- (n=12) and IPF- (n=31) lung tissues by qRT-PCR.



Supplementary-Figure S4: Induction of class-I-histone deacetylases HDAC2 and HDAC3 in fibroblast foci and abnormal bronchiolar epithelium of idiopathic pulmonary fibrosis (IPF)-lungs.

(A) Representative immunohistochemistry for prosurfactant protein-C (proSP-C), HDAC2, HDAC3 and cytokeratin-5 (KRT5) in serial sections of IPF-lung tissue. In IPF, fibroblast foci (FF) as well as overlying abnormal bronchiolar basal cells (positive for KRT5) indicated strong nuclear induction of HDAC2 and HDAC3. IPF-AECII (indicated by arrows and proSP-C-staining) did neither express HDAC2 nor HDAC3.

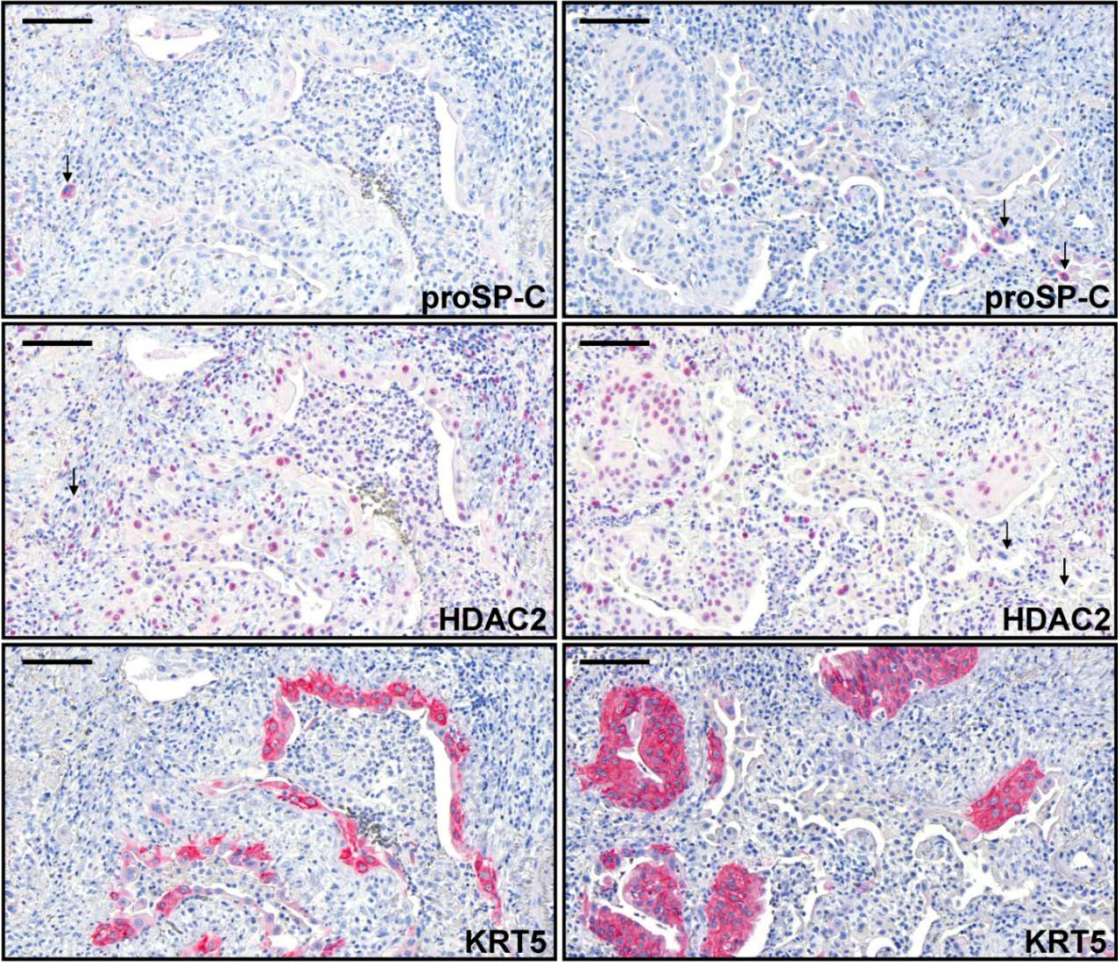
(B) Representative immunohistochemistry for proSP-C, HDAC2, HDAC3 and KRT5 in serial sections of IPF-lung tissue. IPF-AECII (indicated by arrows and proSP-C staining) did neither express HDAC2 nor HDAC3, which were observed to be expressed in the nucleus of ciliated bronchial cells in the very same IPF-lung section. Furthermore, "normal-sized", small bronchiolar basal cells (indicated by dashed arrows and KRT5-staining) in IPF-lungs did neither express HDAC2 nor HDAC3.



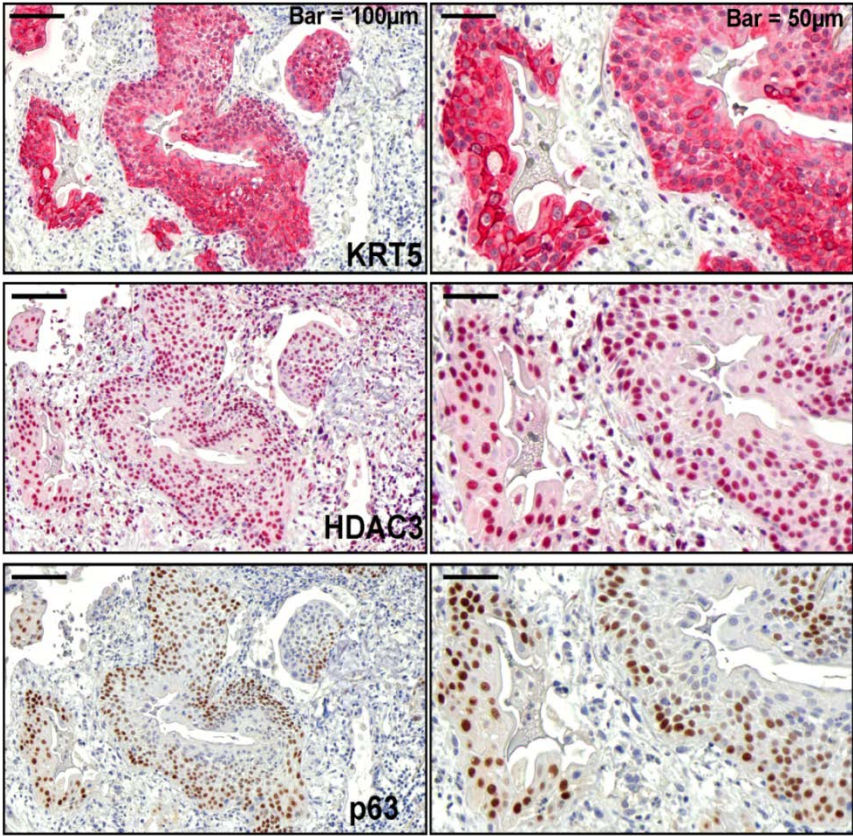
Supplementary-Figure S4C: Nuclear induction of class-I-histone deacetylases HDAC2 and HDAC3 in fibroblast foci and abnormal bronchiolar epithelium of idiopathic pulmonary fibrosis (IPF)-lungs.

Representative immunohistochemistry for HDAC2, HDAC3 and cytokeratin-5 (KRT5) in serial sections of IPF-lung tissue. In IPF, fibroblast foci (FF) as well as overlying abnormal bronchiolar basal cells (positive for KRT5) indicated strong nuclear induction of HDAC2 and HDAC3. The figures in the lower panel represent higher resolution images of supplementary figure S4A.

A



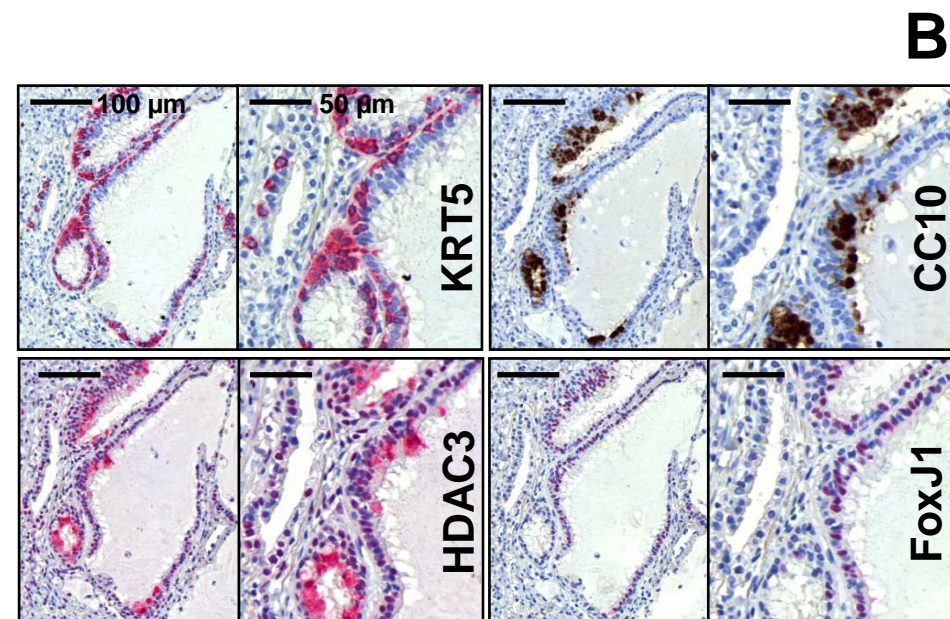
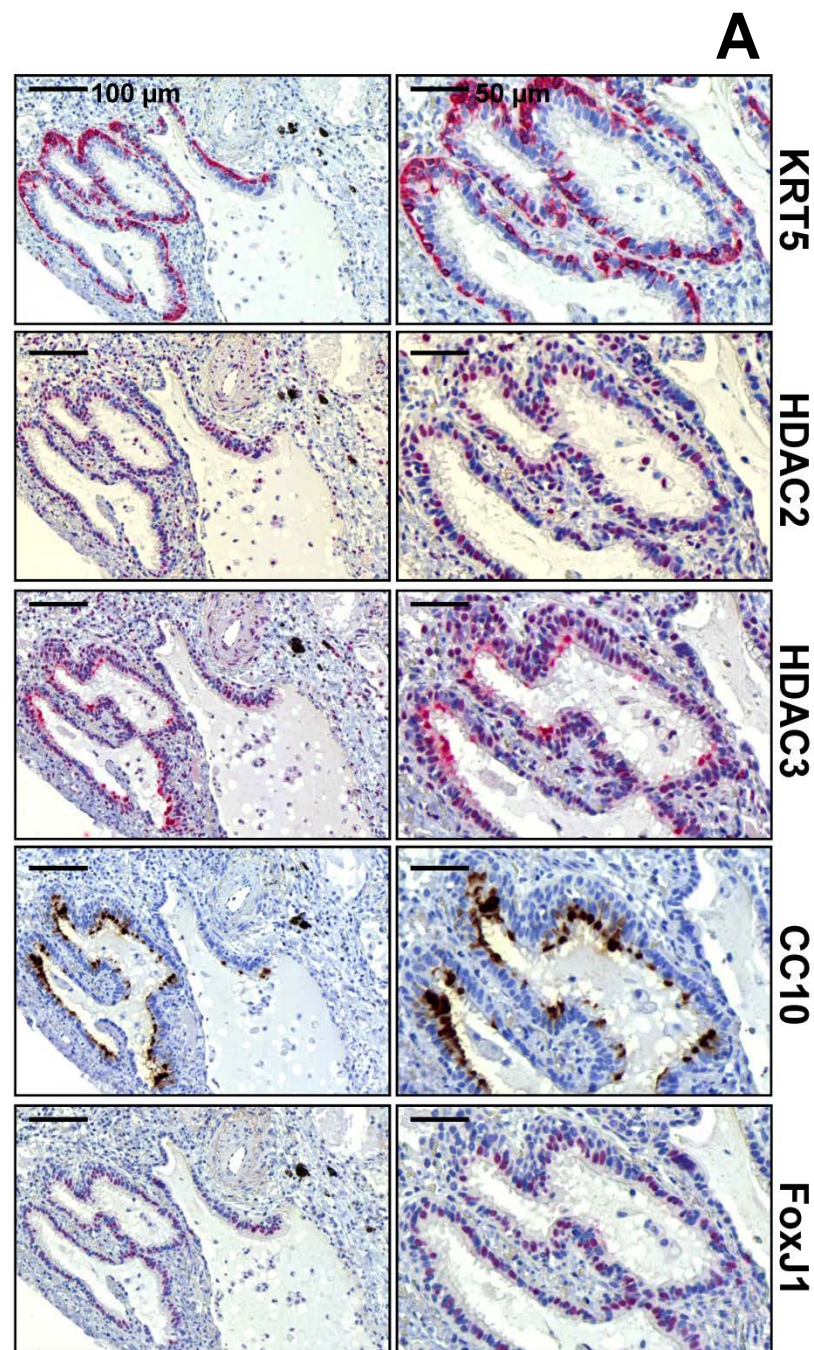
B



Supplementary-Figure S5: Induction of class-I-histone deacetylases HDAC2 and HDAC3 in hyperplastic bronchiolar basal cells in abnormal bronchiolar structures of idiopathic pulmonary fibrosis (IPF)-lungs.

(A) Representative immunohistochemistry for proSP-C, HDAC2, and KRT5 in serial sections of IPF-lung tissue. In IPF, induction of nuclear HDAC2 expression was observed in "hyperplastic" bronchiolar basal cells as well as in basal cell layers of squamous metaplasia (indicated by KRT5-staining) in areas of advanced bronchiolization. IPF-AECII (indicated by arrows and proSP-C-staining) did not express HDAC2.

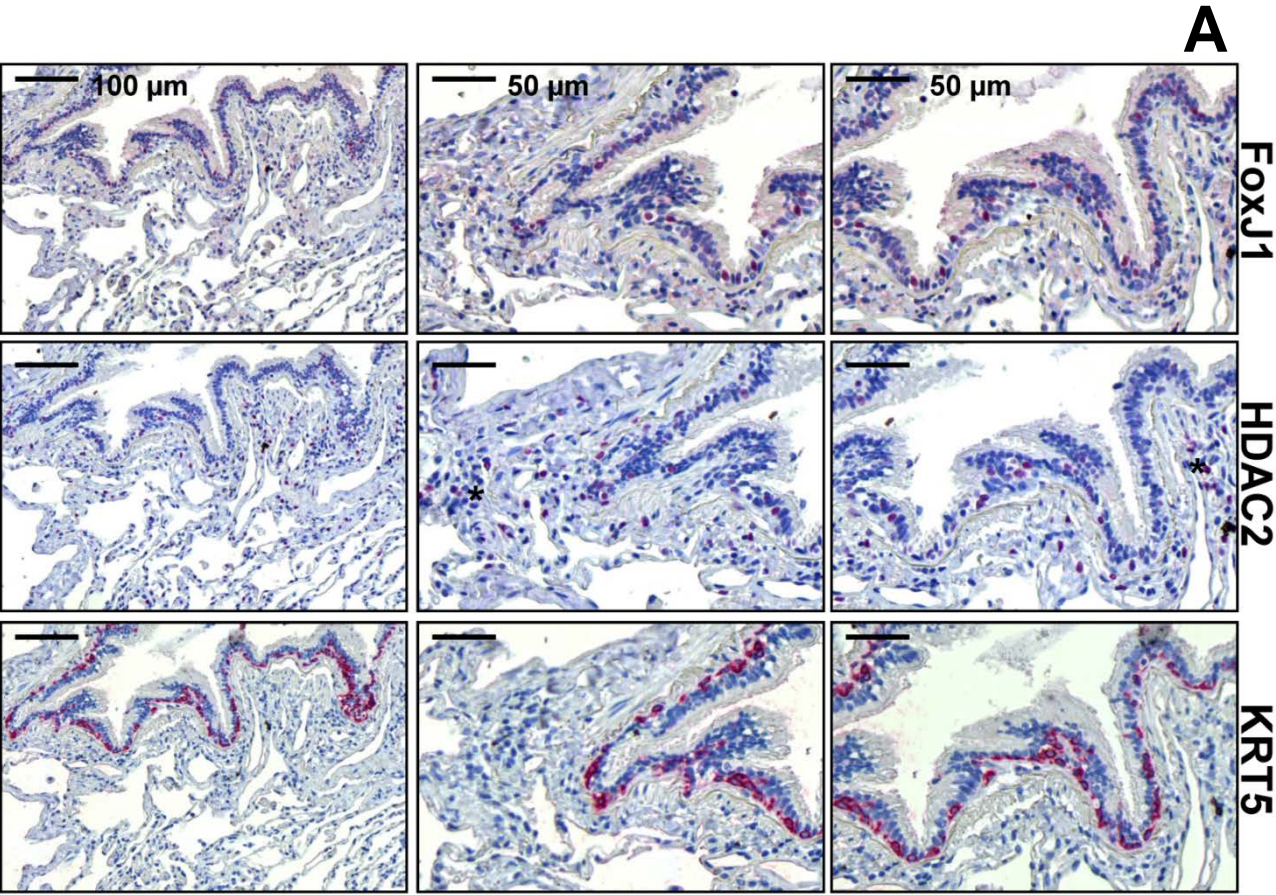
(B) Representative immunohistochemistry for HDAC3, KRT5 and p63 in serial sections of IPF-lung tissue. In IPF, strong nuclear induction of HDAC3 was observed in bronchiolar basal cell sheets of squamous metaplasia (indicated by KRT5 - and nuclear p63-staining) in areas of advanced bronchiolization.



Supplementary-Figure S6: Overexpression of class-I-histone deacetylases HDAC2 and HDAC3 in ciliated bronchial cells in idiopathic pulmonary fibrosis (IPF) lungs. Cytoplasmic expression of HDAC3 in Clara cells of idiopathic pulmonary fibrosis (IPF)-lungs.

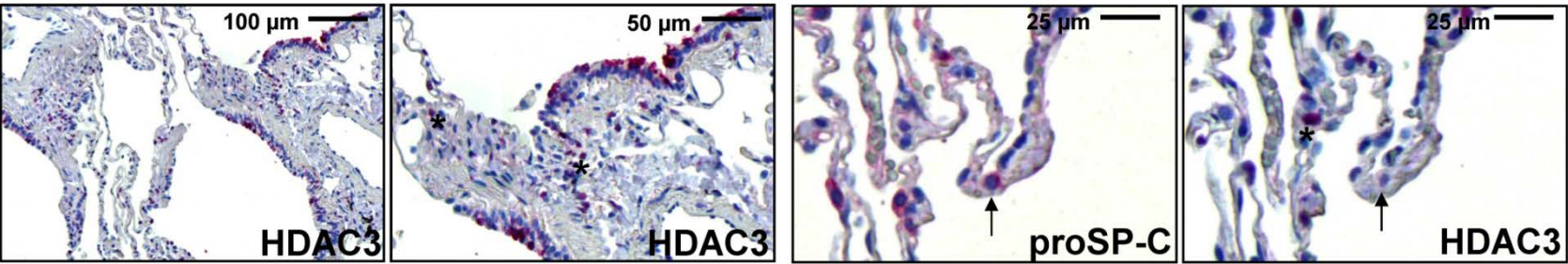
(A) Representative immunohistochemistry for KRT5, HDAC2, HDAC3, Clara Cell-protein 10 (CC10), and Forkhead box protein J1 (FoxJ1) in serial sections of IPF-lung tissue. Ciliated bronchial cells in IPF-lungs (indicated by FoxJ1-staining) revealed strong nuclear expression of HDAC2 and HDAC3. Additionally, non-ciliated Clara cells (positive for CC10) revealed strong cytoplasmic expression of HDAC3, but not of HDAC2.

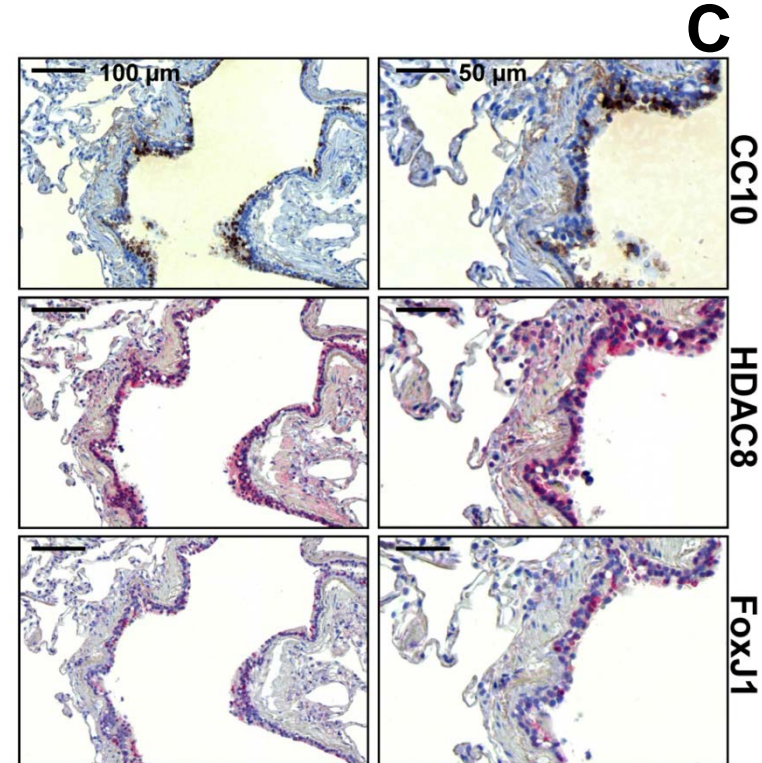
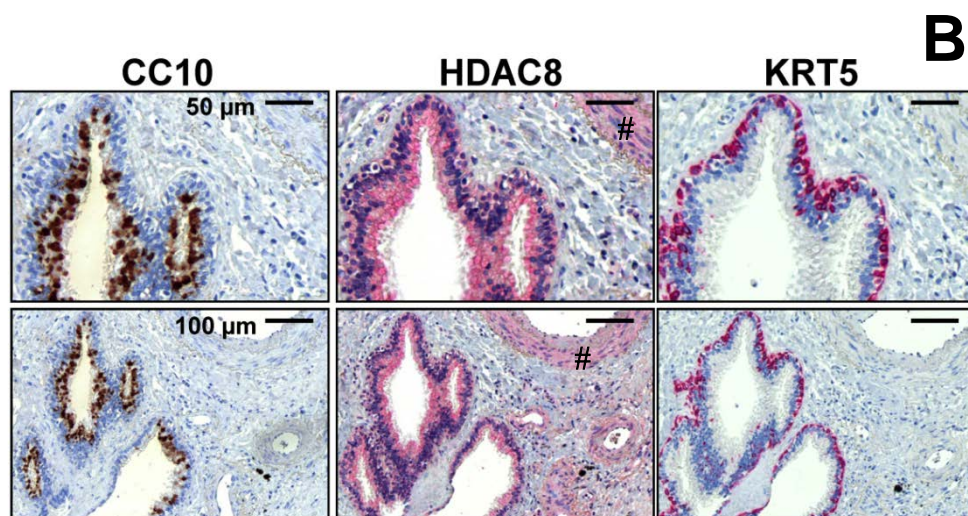
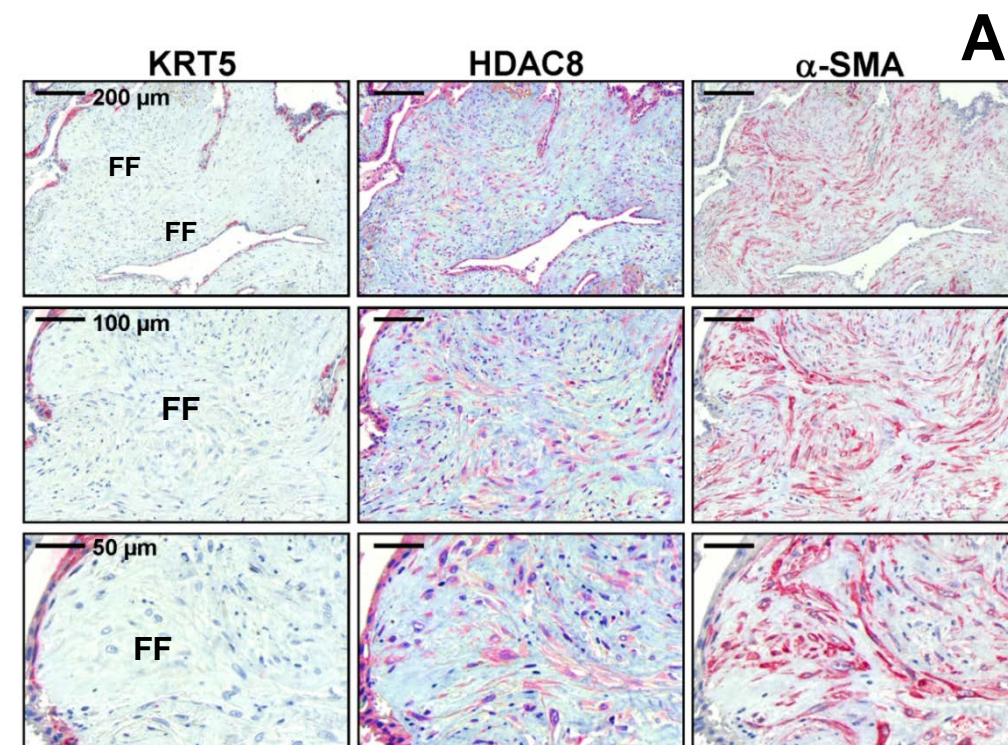
(B) Representative immunohistochemistry for KRT5, HDAC3, CC10, and FoxJ1 in serial sections of IPF-lung tissue.



Supplementary-Figure S7: Expression of class-I-histone deacetylases HDAC2 and HDAC3 in normal control-lungs.

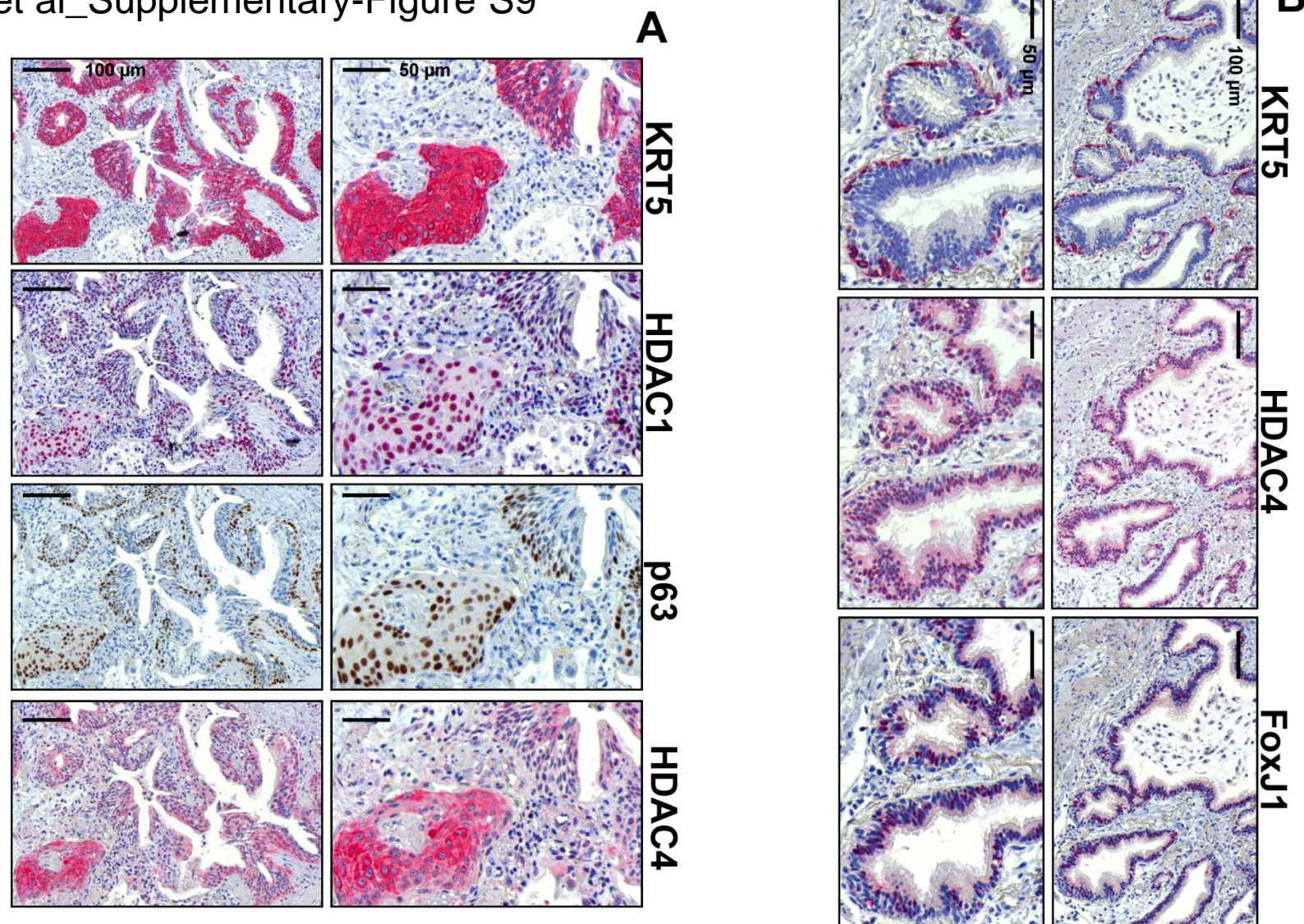
(A) Representative immunohistochemistry for proSP-C, HDAC2 and KRT5 in serial sections of control-lung tissue. "Normal-sized", small basal cells in normal bronchioles of control-lungs indicated no staining for HDAC2 and HDAC3 (not shown). Similarly, ciliated bronchial cells of normal control-lungs indicated no or only faint expression of HDAC2 and HDAC3 (not shown). Only few cells in the interstitium (presumably interstitial inflammatory cells, indicated by asterisks) of control-lungs expressed HDAC2 in the nucleus. (B) Representative immunohistochemistry for HDAC3 and proSP-C in serial sections of control-lung tissue. Clara Cells of control-lungs indicated robust cytoplasmic expression of HDAC3 (left panel), whereas type-II alveolar epithelial cells (AECII, indicated by arrows and proSP-C staining) did not express HDAC3 (right panel). Single interstitial cells in normal lungs (presumably interstitial inflammatory cells, indicated by asterisks) revealed strong nuclear expression of HDAC3.





Supplementary-Figure S8: Expression of class-I-histone deacetylase HDAC8 in idiopathic pulmonary fibrosis (IPF)- and control-lungs.

(A) Representative immunohistochemistry for KRT5, HDAC8 and α -SMA in serial sections of IPF-lung tissue. In IPF, fibroblast foci (FF) as well as overlying abnormal bronchiolar basal cells (positive for KRT5) indicated cytoplasmic expression of HDAC8. (B) Representative immunohistochemistry for CC10, HDAC8 and KRT5 in serial sections of IPF-lung tissue. In IPF, cytoplasmic expression of HDAC8 was observed in bronchiolar basal cells (positive for KRT5), Clara cells (positive for CC10) as well as in ciliated bronchial cells. In addition, vascular smooth muscle cells (VSMCs, indicated by hashmark) showed also cytoplasmic staining for HDAC8. (C) Representative immunohistochemistry for CC10, HDAC8 and FoxJ1 in serial sections of control-lung tissue. Robust expression of HDAC8 was observed in Clara cells (positive for CC10) as well as in ciliated bronchial cells (positive for FoxJ1) of control-lungs.



Supplementary-Figure S9: Expression and localization of class-I-histone deacetylase HDAC1 and Class-IIa-histone deacetylase HDAC4 in idiopathic pulmonary fibrosis (IPF)-lungs.

(A) Representative immunohistochemistry for KRT5, HDAC1, p63 and HDAC4 in serial sections of IPF-lung tissue. Bronchiolar basal cell layers of squamous metaplasia (indicated by KRT5- and nuclear p63-staining) in areas of advanced bronchiolization of IPF-lungs indicated a predominantly cytoplasmic expression of HDAC4, and a nuclear expression of HDAC1.

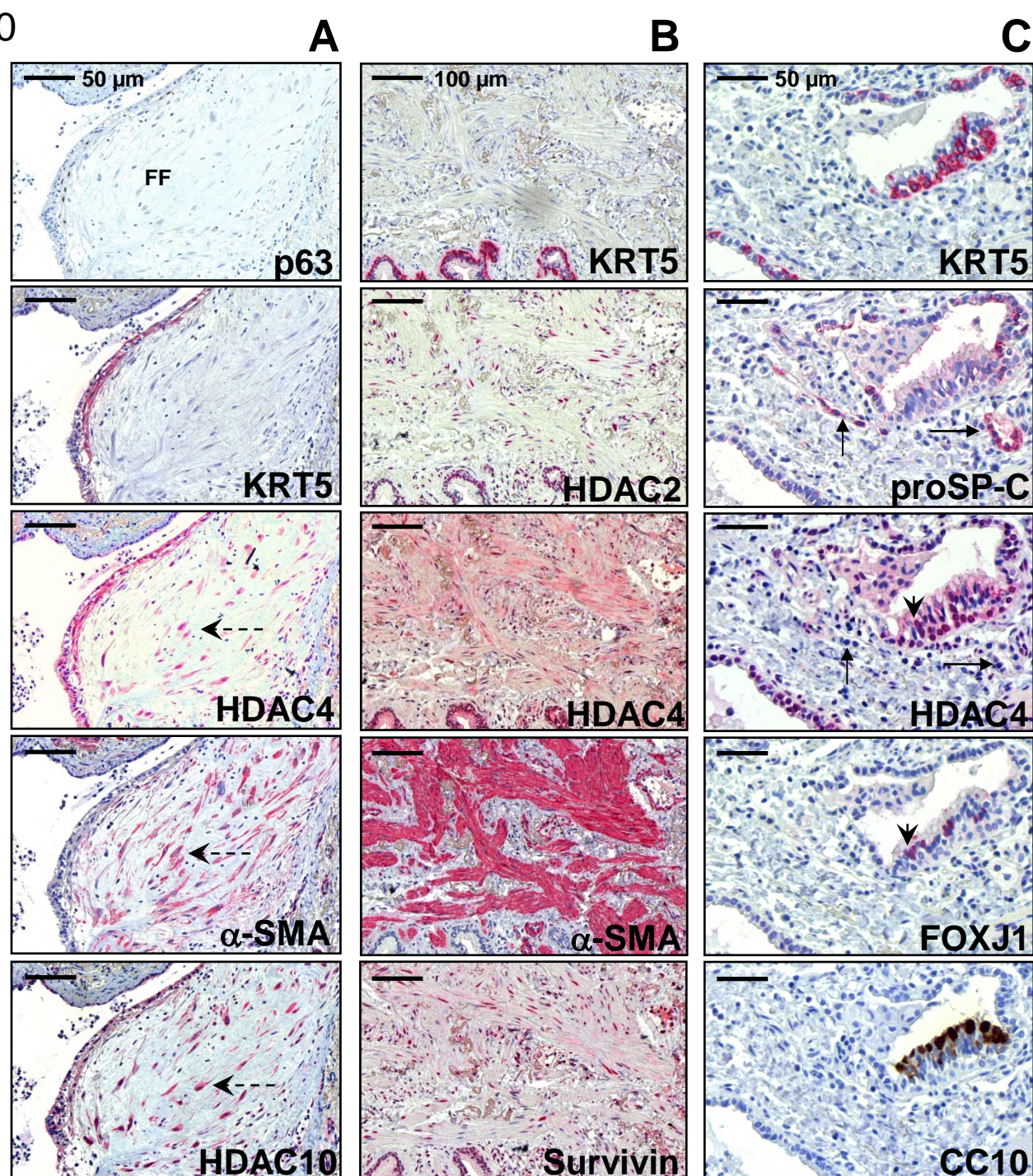
(B) Representative immunohistochemistry for KRT5, HDAC4 and FoxJ1 in serial sections of IPF-lung tissue. Ciliated bronchial cells in abnormal bronchioles of IPF-lungs (marked by FoxJ1-staining) indicated strong nuclear (and weak cytoplasmic) staining for HDAC4.

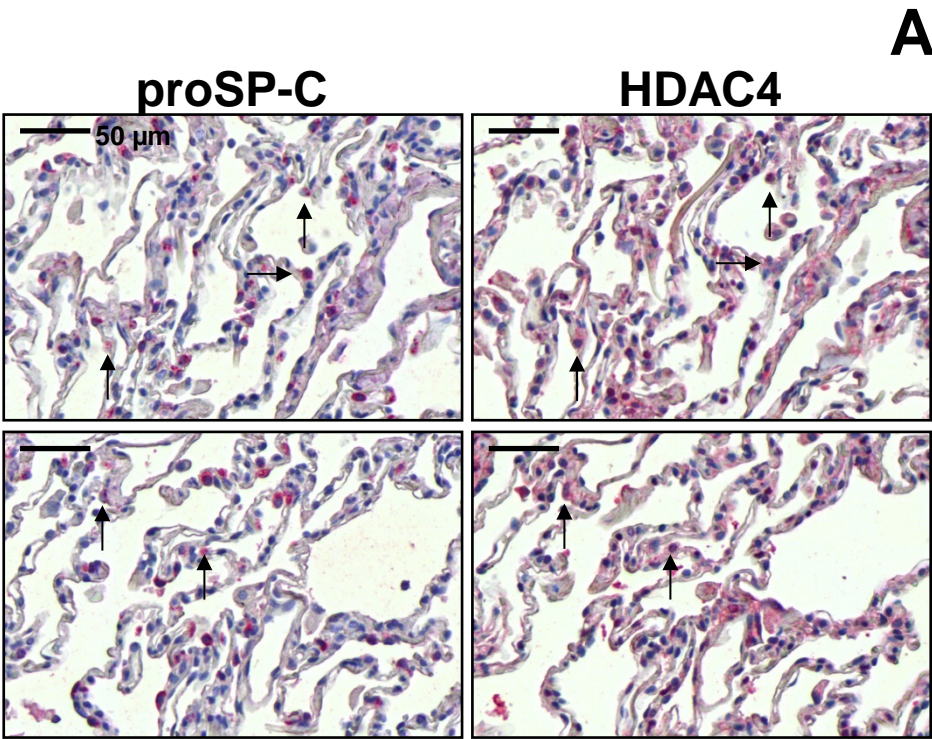
Supplementary-Figure S10: Expression and localization of Class-IIa-histone deacetylase HDAC4 in idiopathic pulmonary fibrosis (IPF)-lungs.

(A) Representative immunohistochemistry for p63, KRT5, HDAC4, α -SMA and HDAC10 in serial sections of IPF-lung tissue. Myofibroblastic cells of fibroblast foci (indicated by dashed arrows) as well as overlying abnormal bronchiolar basal cells (indicated by KRT5- and nuclear p63-staining) showed a predominantly cytoplasmic expression of HDAC4. In addition, HDAC10 was expressed in the nucleus and cytoplasm of myofibroblasts.

(B) Representative immunohistochemistry for KRT5, HDAC2, HDAC4, α -SMA and survivin in serial sections of IPF-lung tissue. HDAC4 indicated a marked cytoplasmic expression in the "mature" smooth muscle in areas of dense, older fibrosis, thereby co-localizing with nuclear HDAC2- and survivin expression.

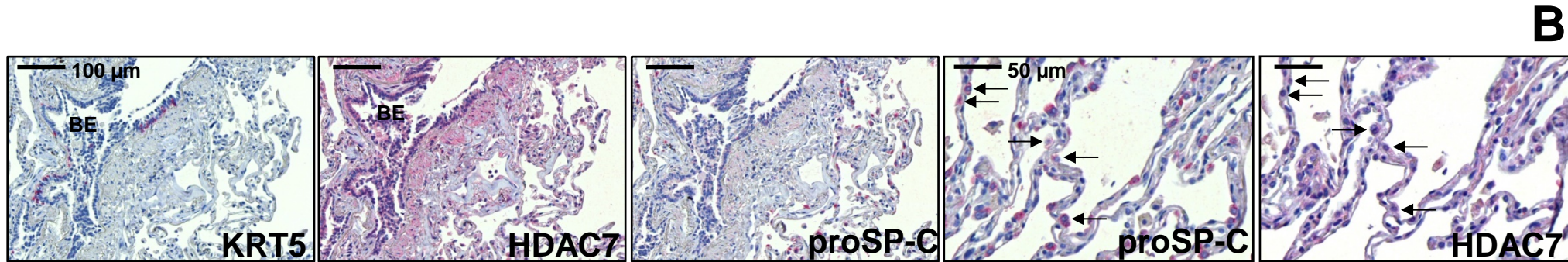
(C) Representative immunohistochemistry for KRT5, proSP-C, HDAC4, Forkhead box protein J1 (FOXJ1) and Clara cell-protein-10 (CC10) in serial sections of IPF-lung tissue. In IPF, strong nuclear staining for HDAC4 is observed in ciliated bronchial cells (indicated by arrowheads and FOXJ1 staining) and basal cells (positive for KRT5) of abnormal hyperplastic bronchioles. Type-II alveolar epithelial cells (AECII, indicated by arrows and proSP-C-staining) and Clara cells (positive for CC10) in IPF-lungs did not express HDAC4.

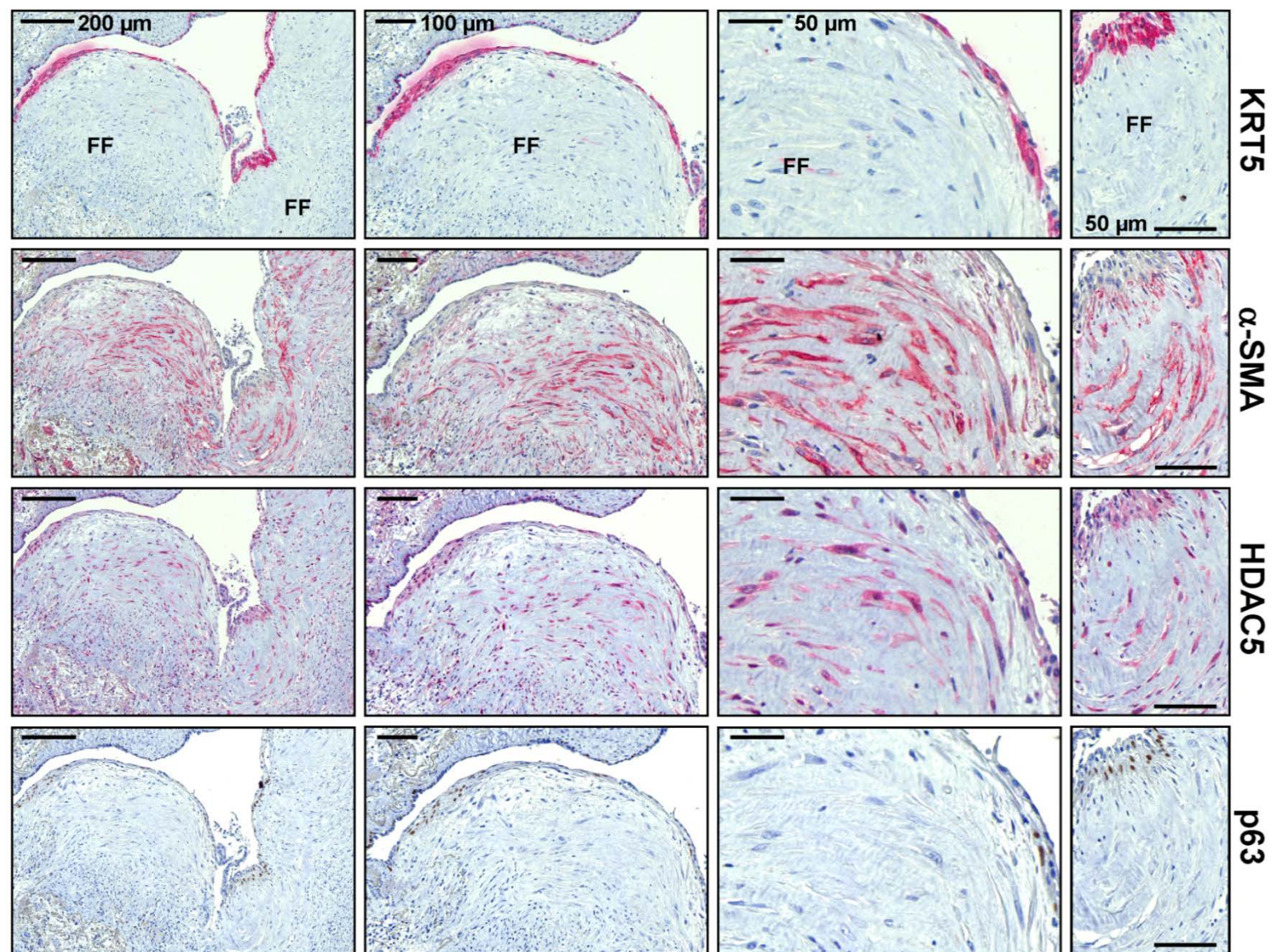




Supplementary-Figure S11: Expression and localization of class-IIa-histone deacetylases HDAC4 and HDAC7 in normal control-lungs.

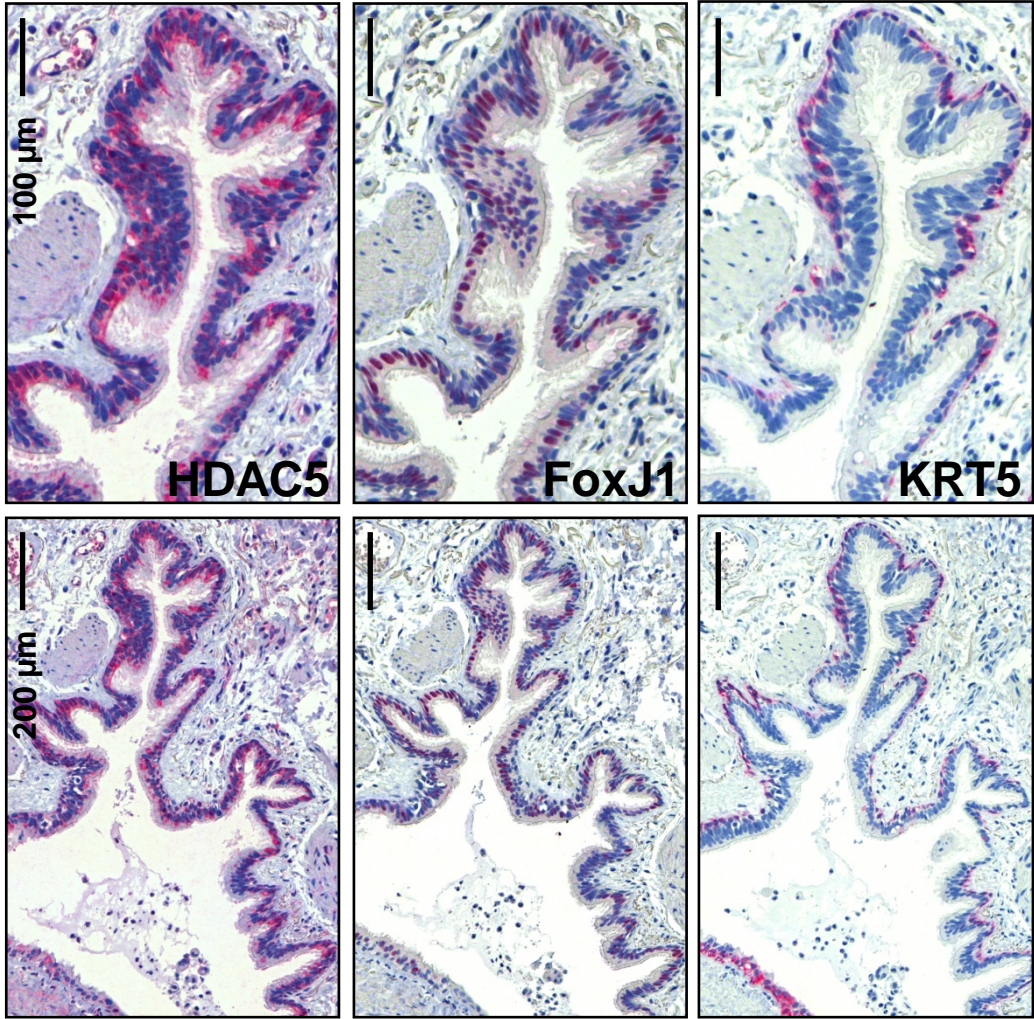
(A) Representative immunohistochemistry for HDAC4 and proSP-C in serial sections of control donor-lungs. In the normal lung, HDAC4 is expressed in the nucleus of type-II alveolar epithelial cells (AECII, indicated by arrows and proSP-C staining). (B) Representative immunohistochemistry for KRT5, HDAC7, and proSP-C in serial sections of control-lung tissue. In control-lungs, moderate expression for HDAC7 is observed in bronchial epithelium (BE); AECII in normal lungs (indicated by arrows and proSP-C staining) revealed faint cytoplasmic HDAC7 expression.



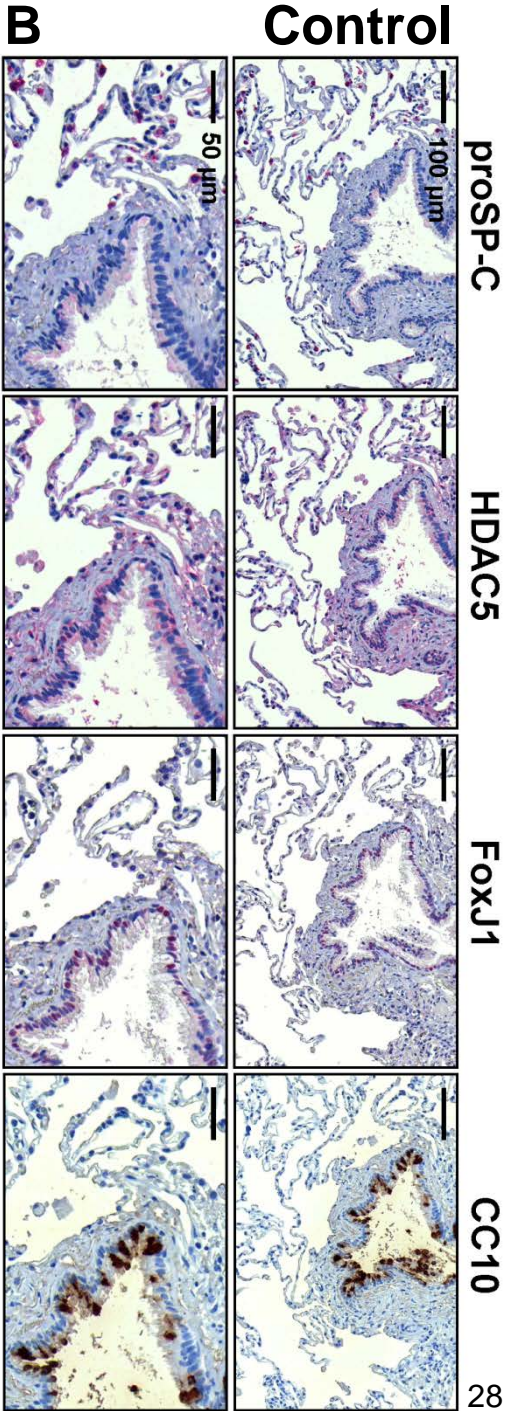


Supplementary-Figure S12: Induction of class-IIa-histone deacetylase HDAC5 in fibroblast foci and abnormal bronchiolar epithelium of idiopathic pulmonary fibrosis (IPF)-lungs.

Representative immunohistochemistry for KRT5, α -SMA, HDAC5 and p63 in serial sections of IPF-lung tissue. In IPF, the antibody for HDAC5 revealed cytoplasmic staining of myofibroblasts in fibroblast foci [FF] (indicated by α -SMA-staining of serial sections) and in overlying hyperplastic bronchiolar basal cells (positive for KRT5 and p63).



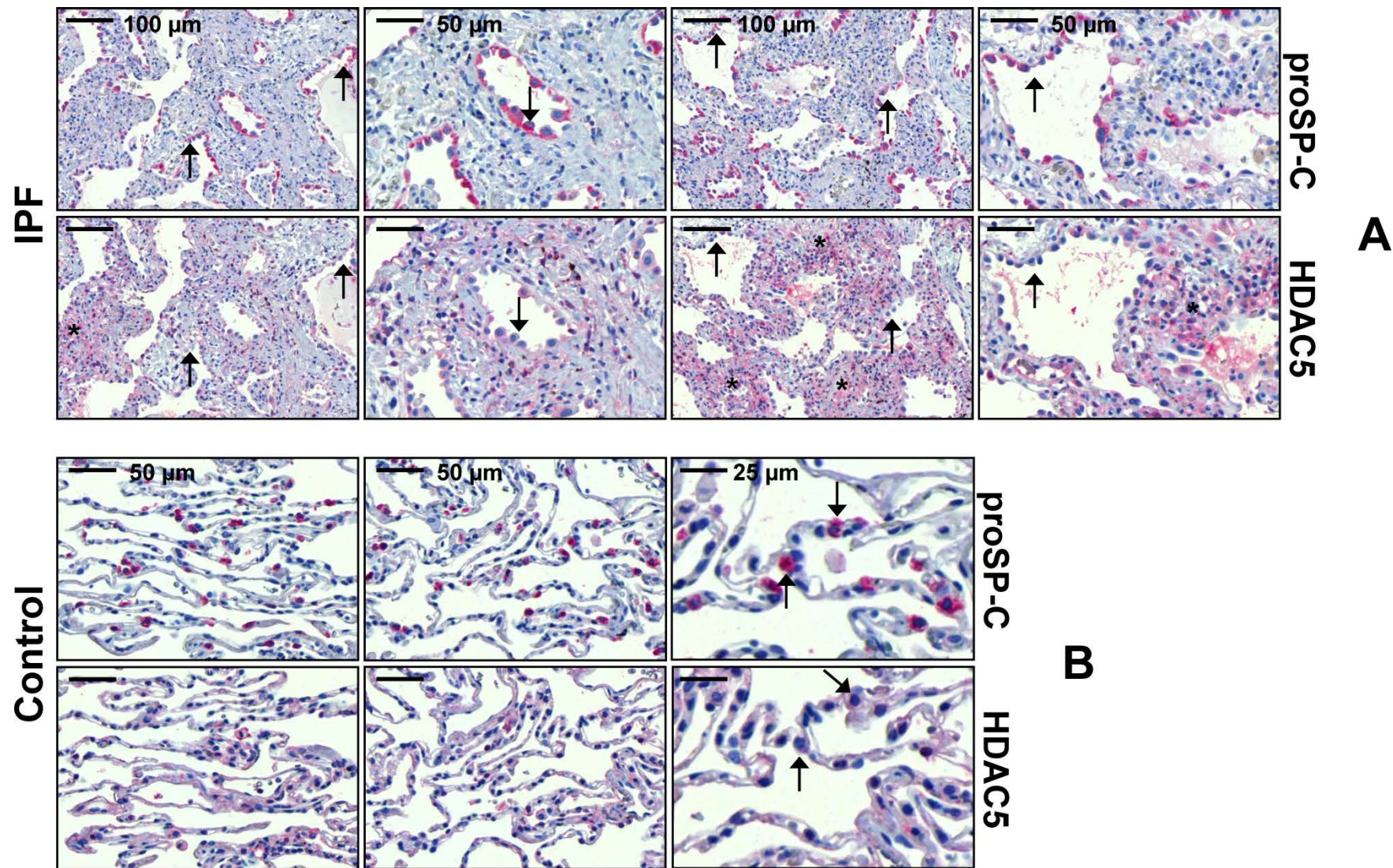
A IPF



Supplementary-Figure S13: Induction and upregulation of class-IIa-histone deacetylase HDAC5 in ciliated bronchial epithelium of idiopathic pulmonary fibrosis (IPF)-lungs.

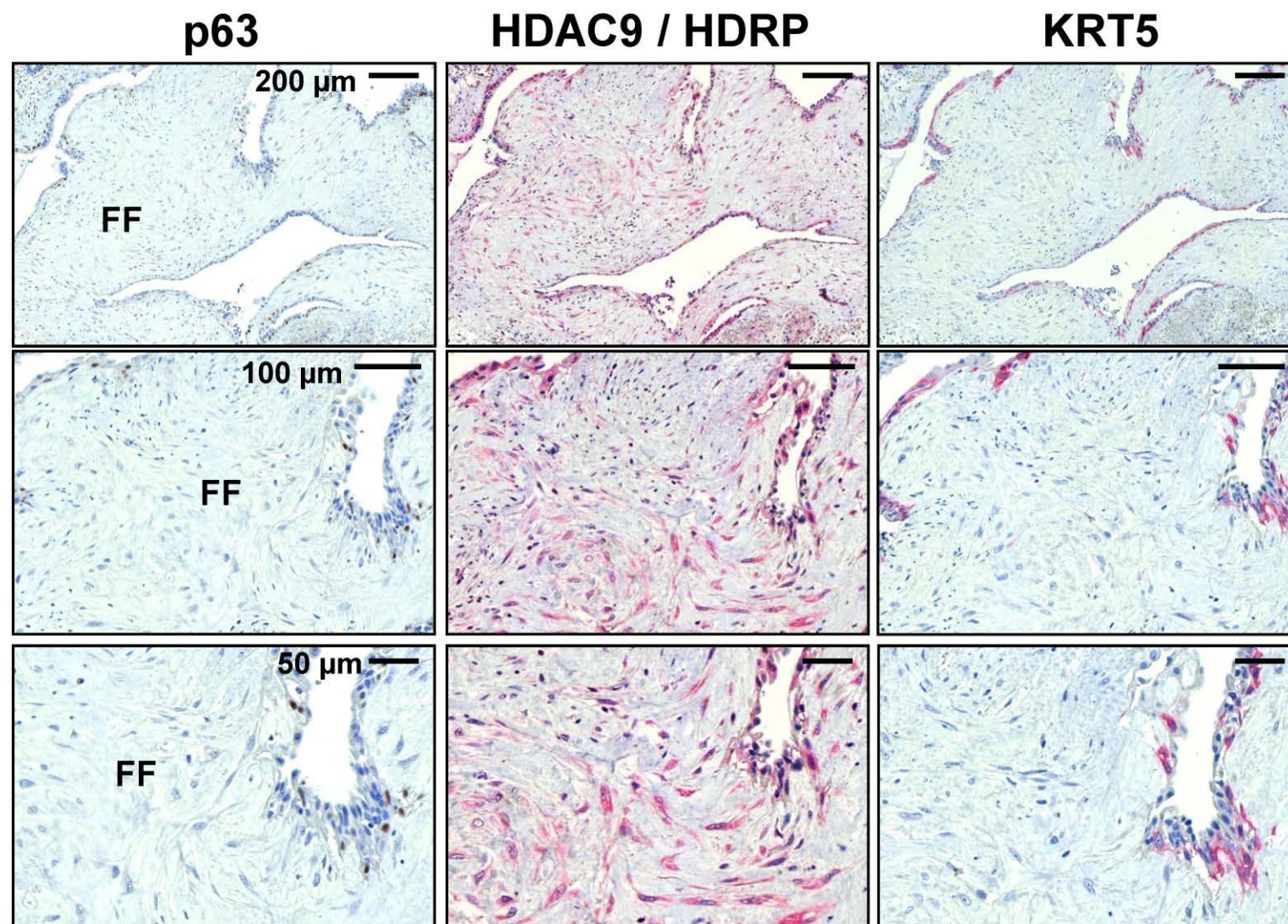
(A) Representative immunohistochemistry for HDAC5, FoxJ1 and KRT5 in serial sections of IPF-lung tissue. Strong cytoplasmic expression of HDAC5 was observed in ciliated bronchial cells (indicated by nuclear FoxJ1-staining) of abnormal bronchioles in IPF-lungs.

(B) Representative immunohistochemistry for proSP-C, HDAC5, FoxJ1 and CC10 in serial sections of control-lung tissue. Ciliated bronchial cells of normal bronchioles in control-lungs (indicated by nuclear FoxJ1-staining) revealed faint cytoplasmic expression of HDAC5. Type-II alveolar epithelial cells (indicated by proSP-C-staining) and Clara cells (positive for CC10) revealed no notable expression of HDAC5.



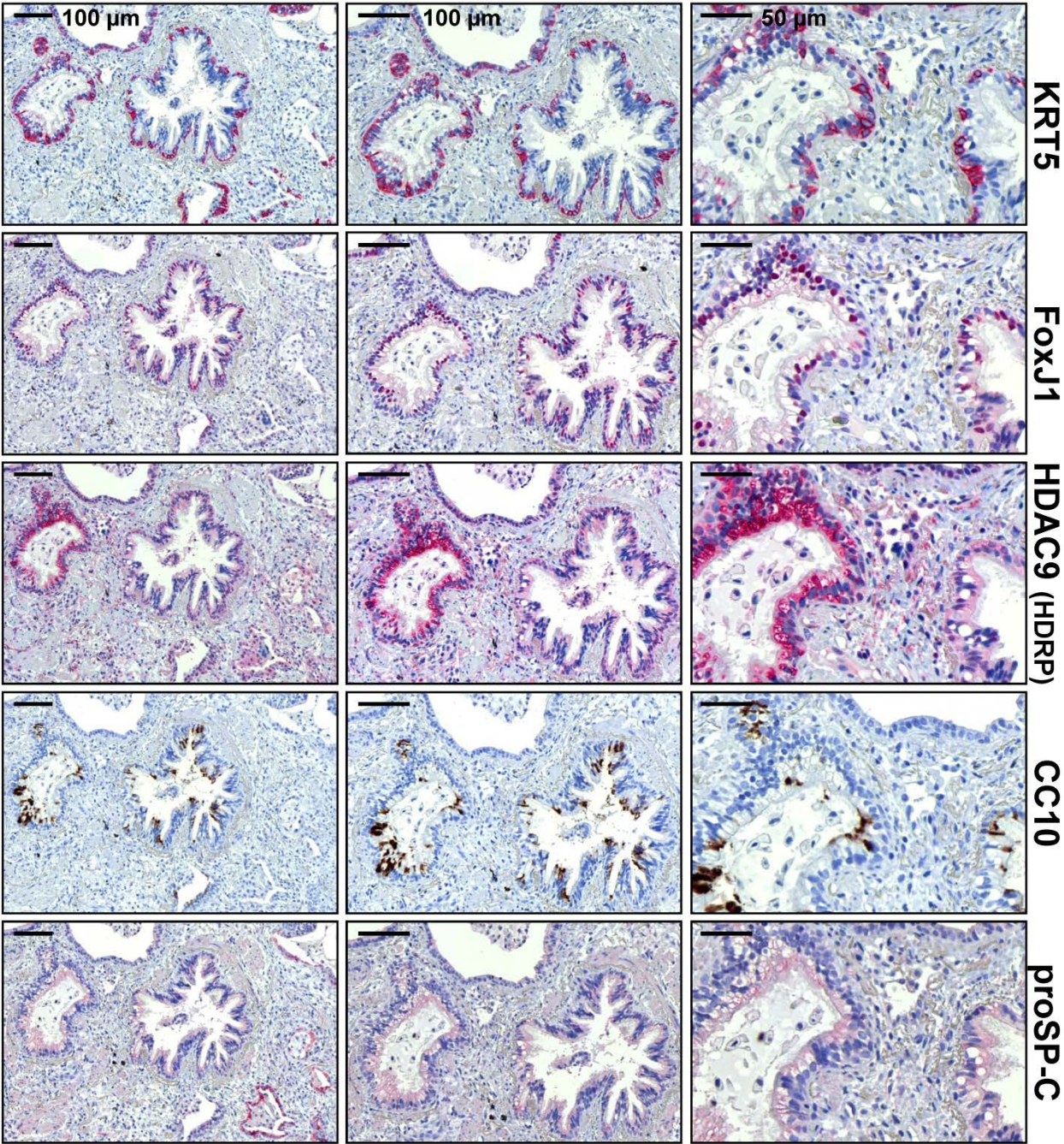
Supplementary-Figure S14: Class-IIa-histone deacetylase HDAC5 is not significantly expressed in type-II alveolar epithelial cells of idiopathic pulmonary fibrosis (IPF)- and control-lungs.

(A) Representative immunohistochemistry for proSP-C and HDAC5 in serial sections of IPF-lung tissue. Type-II alveolar epithelial cells (AECII) of IPF-lungs (indicated by arrows and proSP-C-staining) did not reveal a significant immunostaining for HDAC5. (B) Representative immunohistochemistry for proSP-C and HDAC5 in serial sections of control-lung tissue. AECII of normal lungs (indicated by arrows and proSP-C-staining) did not express HDAC5.



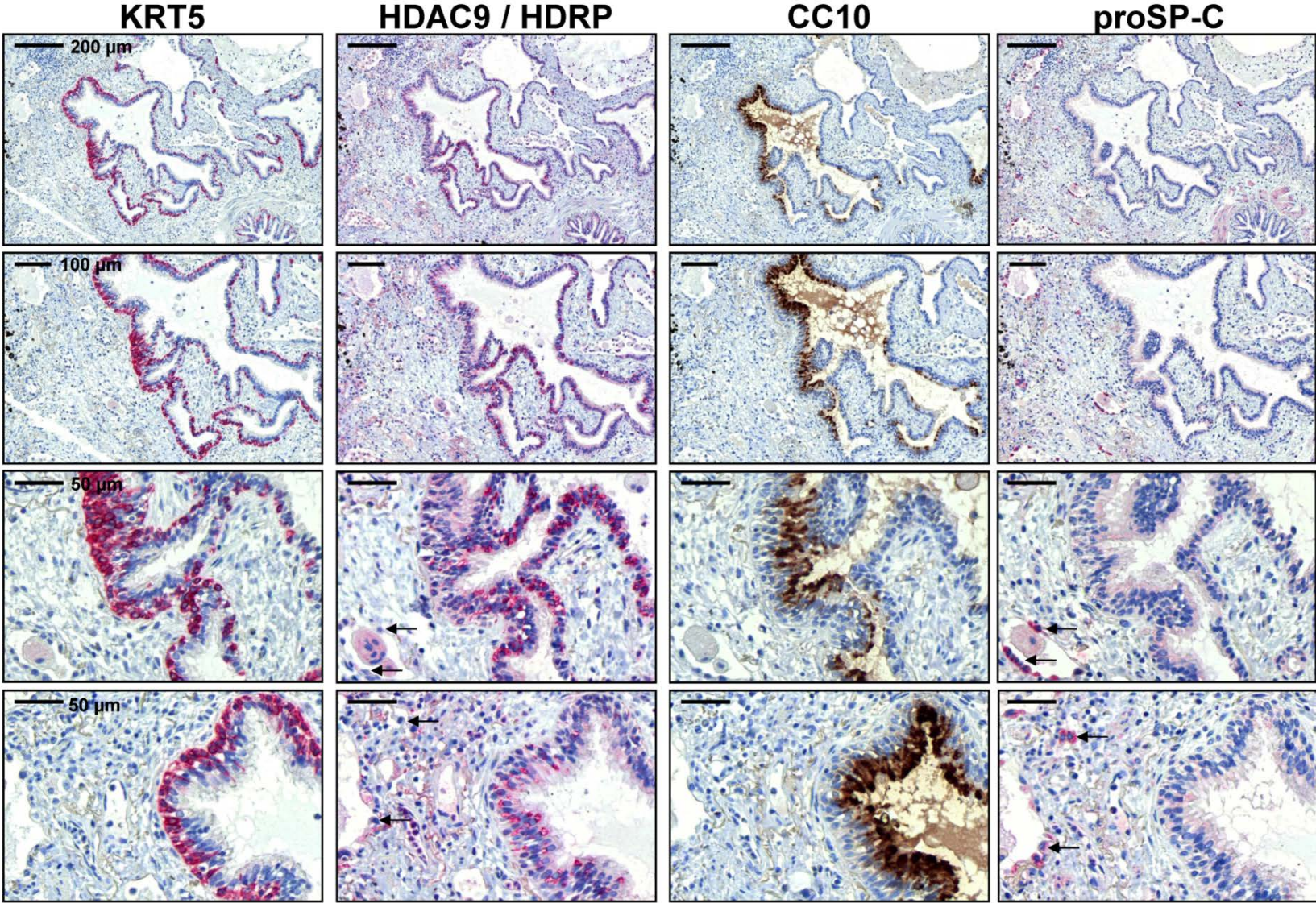
Supplementary-Figure S15: Expression of class-IIa-histone deacetylase HDAC9-isoform HDRP in fibroblast foci and abnormal bronchiolar epithelium of idiopathic pulmonary fibrosis (IPF) lungs.

Representative immunohistochemistry for p63, HDRP, and KRT5 in serial sections of IPF-lung tissue. In IPF, the antibody for HDRP revealed robust cytoplasmic staining of myofibroblasts in fibroblast foci [FF] and in overlying bronchiolar basal cells (indicated by KRT5- and p63-staining).



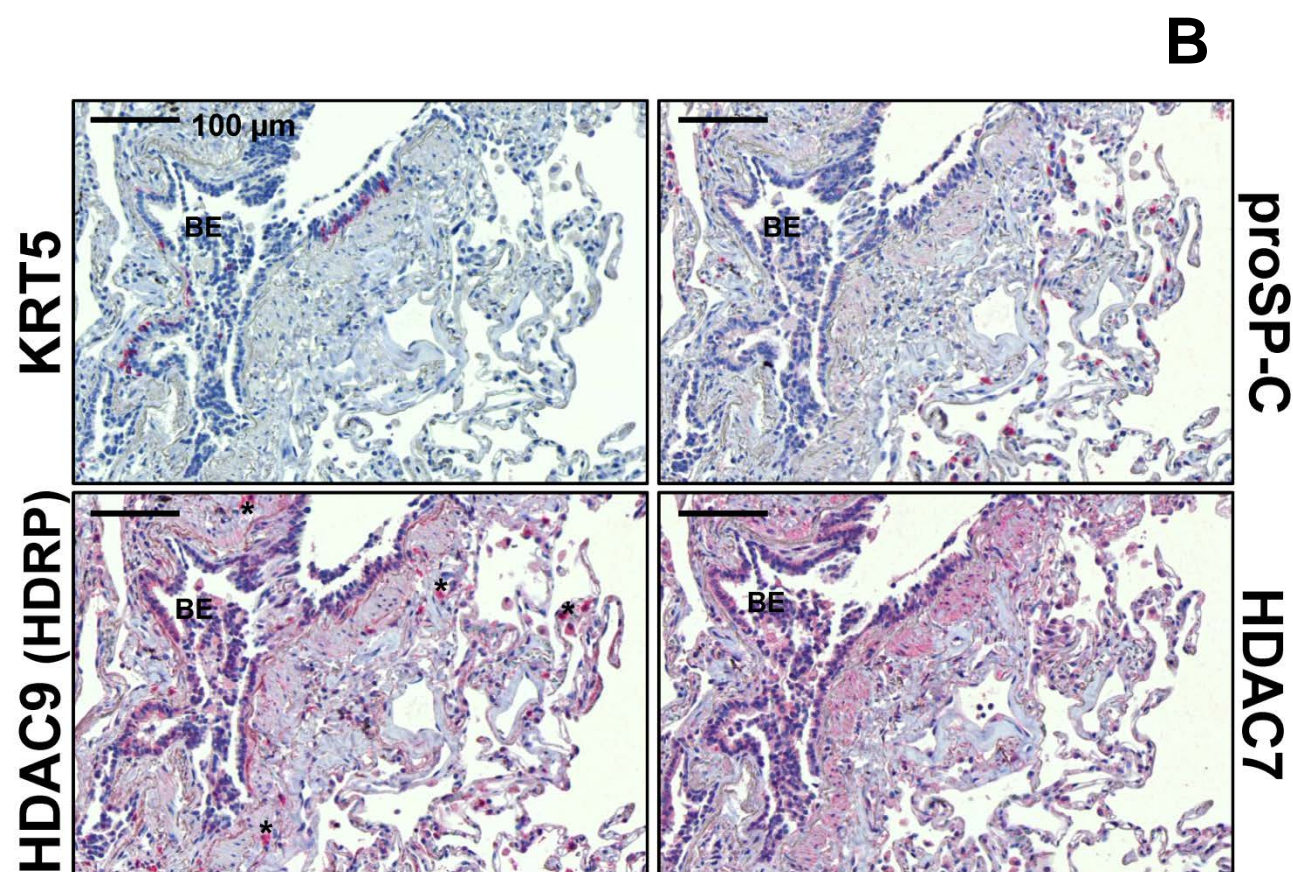
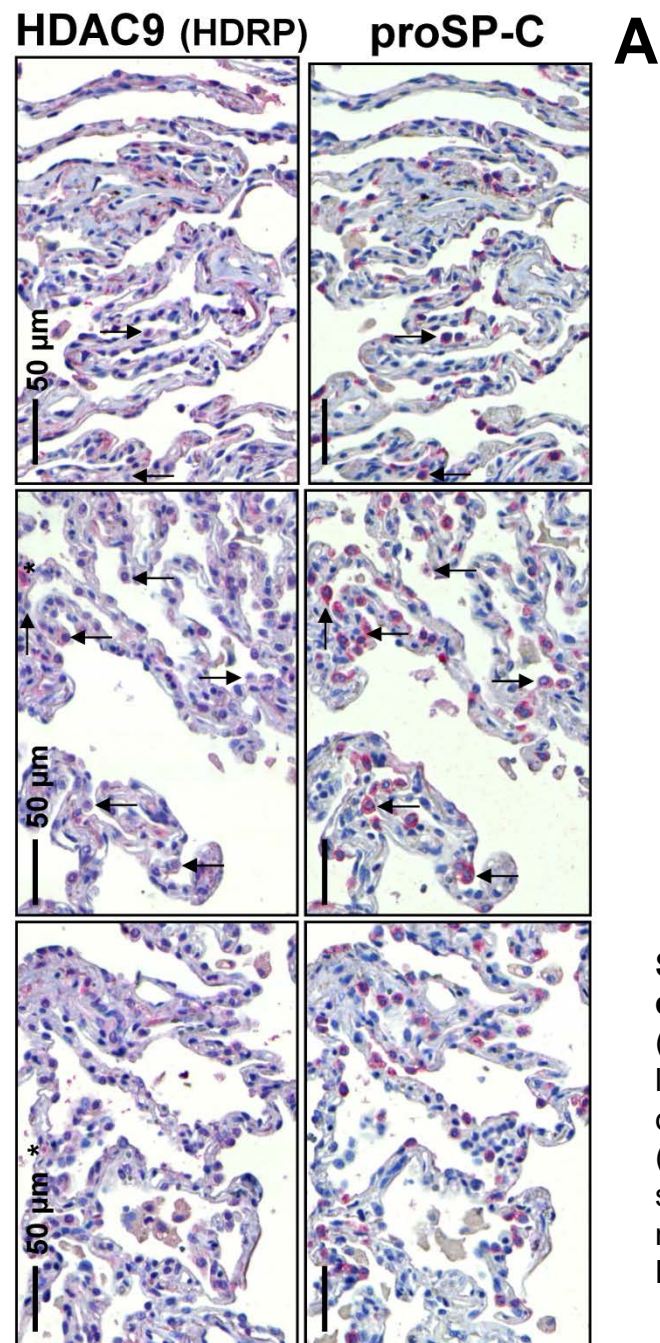
Supplementary-Figure S16: Induction of HDAC9-isoform HDRP in a particular subtype of bronchial epithelial cells of idiopathic pulmonary fibrosis (IPF)-lungs.

Representative immunohistochemistry for KRT5, FoxJ1, HDRP, CC10 and proSP-C in serial sections of IPF-lung tissue. In IPF, the antibody for HDRP revealed robust cytoplasmic staining of a luminal bronchial cell type which was positive for FoxJ1, but not for CC10, and which could never be observed in normal control-lungs. It has to be noted, that not all FoxJ1-positive ciliated bronchial cells of IPF-lungs revealed significant expression of HDRP.



Supplementary-Figure S17: Expression and localization of HDAC9-isoform HDRP in a particular subtype of bronchial epithelial cells of idiopathic pulmonary fibrosis (IPF)-lungs.

Representative immunohistochemistry for KRT5, HDRP, CC10 and proSP-C in serial sections of IPF-lung tissue. In IPF, the antibody for HDRP revealed robust cytoplasmic staining of a luminal bronchial cell type which could never be observed in normal control-lungs. Clara cells (positive for CC10) did not express HDRP, and also bronchiolar basal cells (positive for KRT5) of normal as well as abnormal bronchioles in IPF revealed no or only weak expression of HDRP. AECII in IPF-lungs (indicated by arrows and proSP-C-staining) showed no significant expression of HDRP.

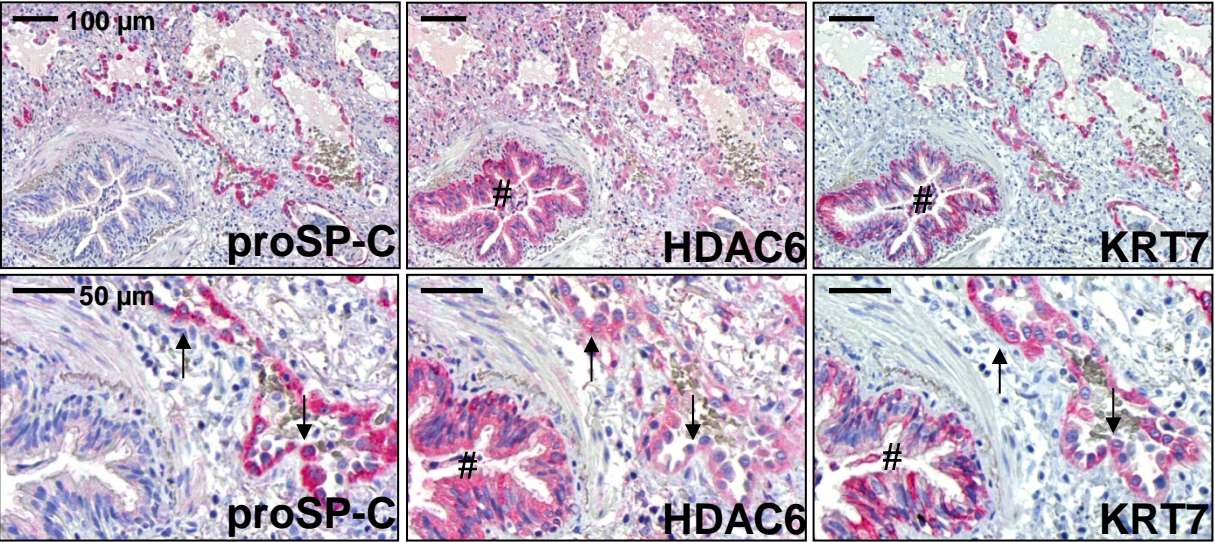


Supplementary-Figure S18: Expression and localization of HDAC9-isoform HDRP in control-lungs.

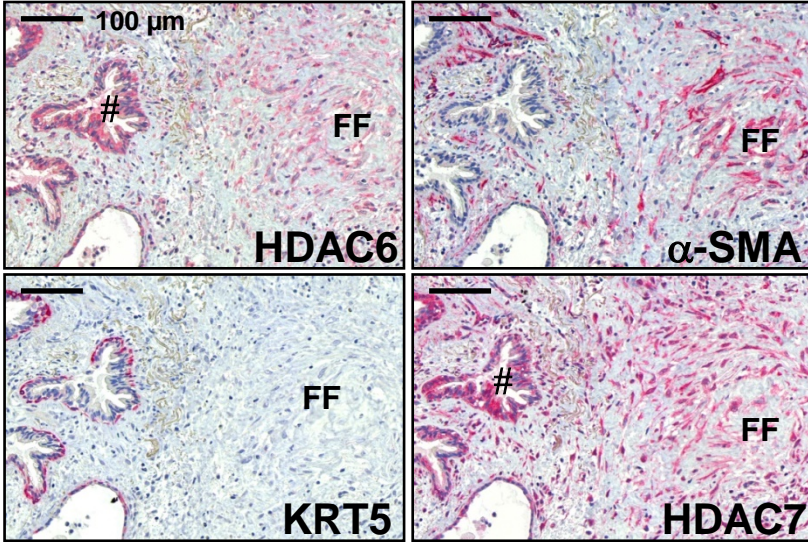
(A) Representative immunohistochemistry for HDRP and proSP-C in serial sections of control-lung tissue. AECII in normal lungs (indicated by arrows and proSP-C-staining) revealed no or only faint expression of HDAC9.

(B) Representative immunohistochemistry for KRT5, HDRP, proSP-C and HDAC7 in serial sections of control-lung tissue. HDRP was weakly expressed in bronchial epithelium (BE) of normal control-lungs. Interstitial inflammatory cells (indicated by asterisks) revealed strong HDRP expression.

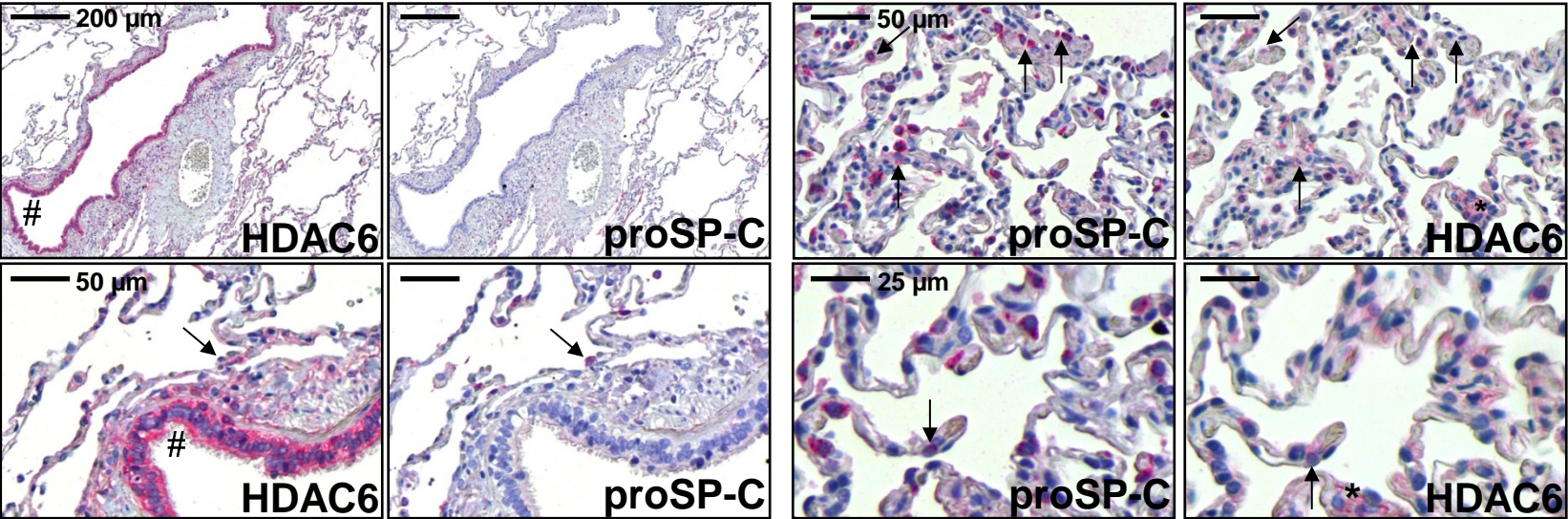
A



B



C

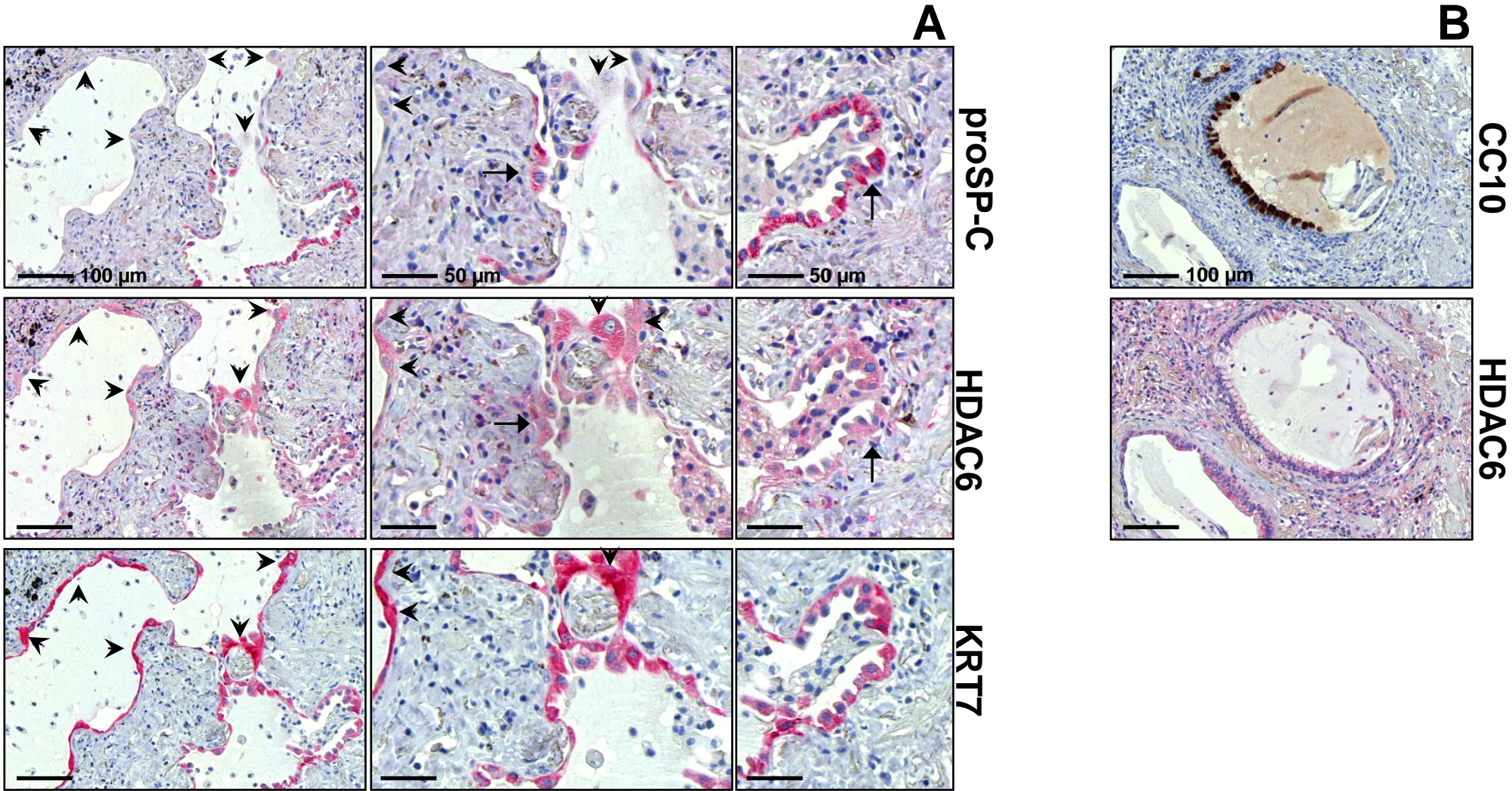


Legend to Supplementary-Figure S19: Expression and localization of Class-IIb-histone deacetylase HDAC6 in idiopathic pulmonary fibrosis (IPF) - and non-diseased control-lungs.

(A) Representative immunohistochemistry for proSP-C, HDAC6, and cytokeratin-7 (KRT7) in serial sections of IPF-lung tissue. In IPF, robust expression of HDAC6 was observed in type-II alveolar epithelial cells (AECII) surrounded by fibrotic tissue (indicated by arrows and proSP-C-staining); and a very strong staining for HDAC6 was observed in ciliated bronchial epithelial cells (indicated by hashmarks and KRT7-staining).

(B) Representative immunohistochemistry for HDAC6, α -SMA, KRT5 and HDAC7 in serial sections of IPF-lung tissue. In IPF, myofibroblasts of fibroblast foci (FF, indicated by α -SMA-staining) revealed moderate expression of HDAC6, in comparison to the very strong HDAC7 expression in FF.

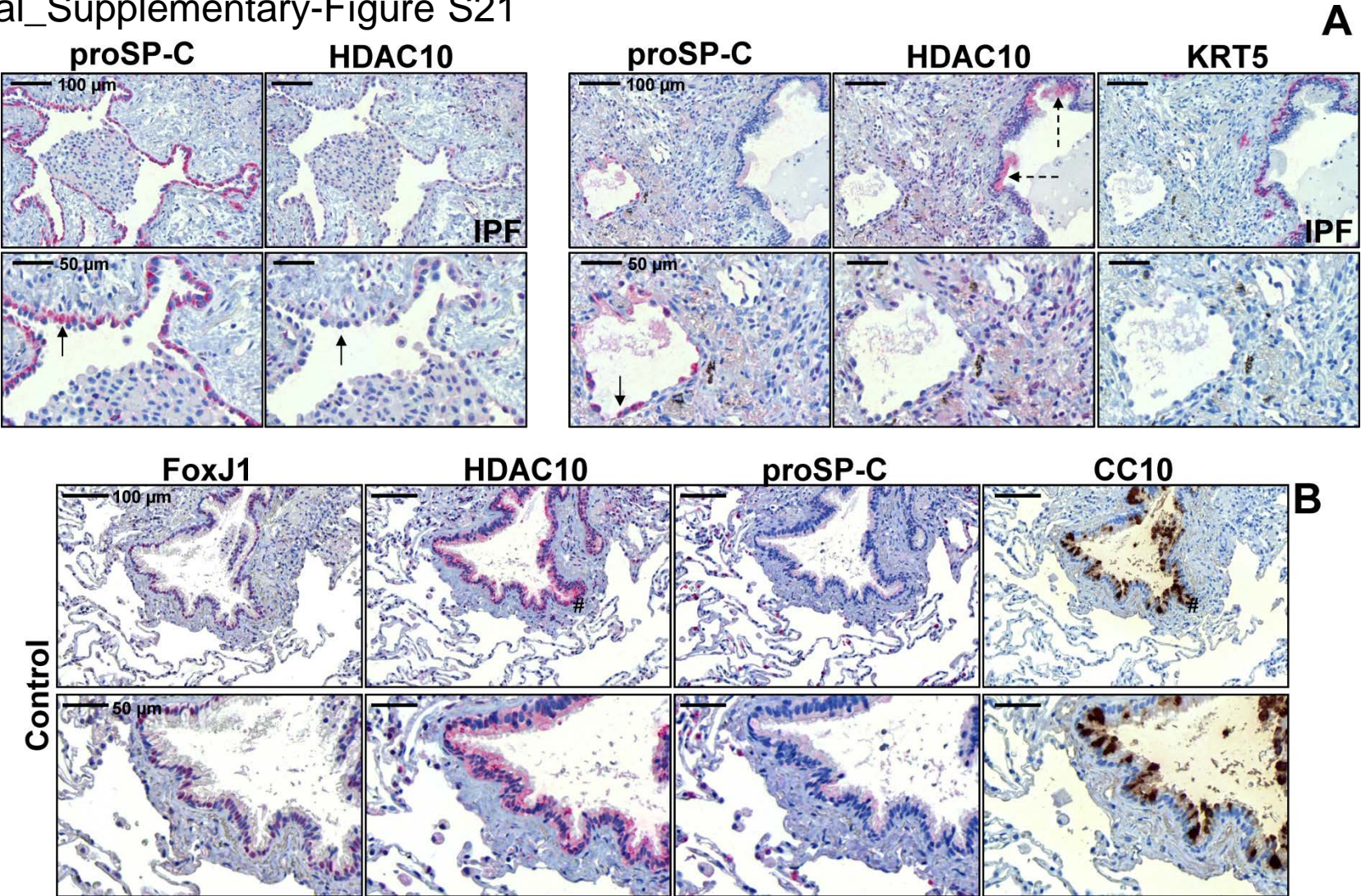
(C) Representative immunohistochemistry for HDAC6 and proSP-C in serial sections of control-lung tissue. In control-lungs, no or weak expression of HDAC6 was observed in AECII (indicated by arrows and proSP-C-staining), whereas the ciliated bronchial epithelium (indicated by hashmarks) revealed very strong HDAC6 expression. Basal expression of HDAC6 was also observed in the interstitium of normal lungs (indicated by asterisks).



Supplementary-Figure S20: Expression and localization of class-IIb-histone deacetylase HDAC6 in idiopathic pulmonary fibrosis (IPF) lungs.

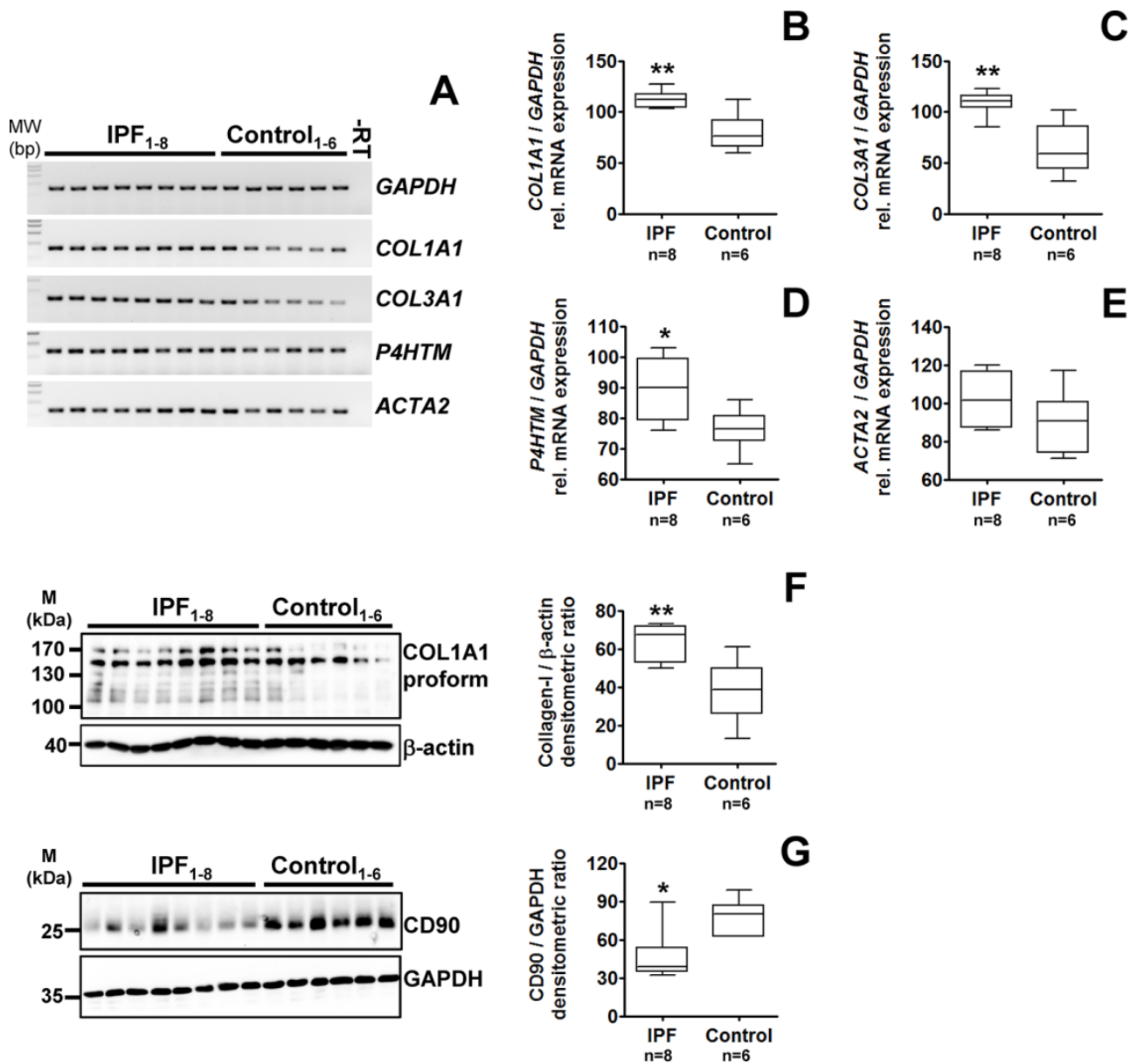
(A) Representative immunohistochemistry for proSP-C, HDAC6, and KRT7 in serial sections of IPF-lung tissue. In IPF, HDAC6 was expressed in the cytoplasm of AECII (indicated by arrows and proSP-C-staining), and in AECII-like cells without proSP-C expression or representing possibly type-I alveolar epithelial cells (indicated by arrowheads and KRT7-staining for indication of simple epithelia).

(B) Representative immunohistochemistry for CC10 and HDAC6 in serial sections of IPF-lung tissue. Clara cells (positive for CC10) in IPF- as well as control-lungs did not express HDAC6.



Supplementary-Figure S21: Expression and localization of class-IIb-histone deacetylase HDAC10 in idiopathic pulmonary fibrosis (IPF)- and control-lungs.

(A) Representative immunohistochemistry for proSP-C, HDAC10, and KRT5 in serial sections of IPF-lung tissue. AECII in IPF-lungs (indicated by arrows and proSP-C-staining) did not express HDAC10. Instead of that, Clara cells (indicated by dashed arrows) revealed robust cytoplasmic expression of HDAC10. Ciliated bronchial cells indicated weak cytoplasmic HDAC10 expression. (B) Representative immunohistochemistry for FoxJ1, HDAC10, proSP-C, and CC10 in serial sections of control-lung tissue. In normal control-lungs, HDAC10 was robustly expressed in non-ciliated Clara cells (indicated by hashmarks and CC10-staining); ciliated bronchial cells (positive for FoxJ1) indicated a weak-to-moderate expression of HDAC10. AECII in control-lungs (indicated by proSP-C-staining) did not indicate a significant HDAC10 expression.

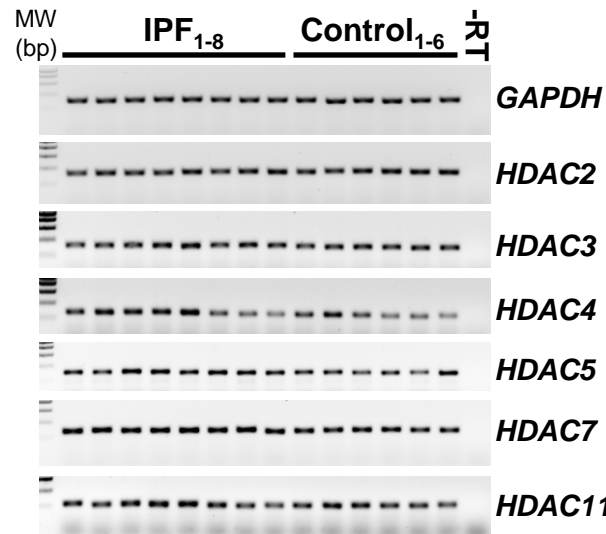


Supplementary-Figure S22: Expression analysis of extracellular matrix (ECM) associated genes in primary fibroblasts isolated from idiopathic pulmonary fibrosis (IPF) - and non-diseased control-lungs.

(A-E) Representative agarose gels (A) and densitometric quantification of reverse transcription-polymerase chain reactions for COL1A1 (B), COL3A1 (C), P4HTM (D), and ACTA2 (E) of human fibroblasts isolated from peripheral explanted lung tissue of patients with IPF (n=8) and non-diseased control-lungs (control, n=6). Each PCR reaction was performed with 100 ng reverse-transcribed complementary DNA, and GAPDH was used as reference gene. -RT control = PCR of a RNA sample without reverse transcriptase. *p<0.05, **p<0.01.

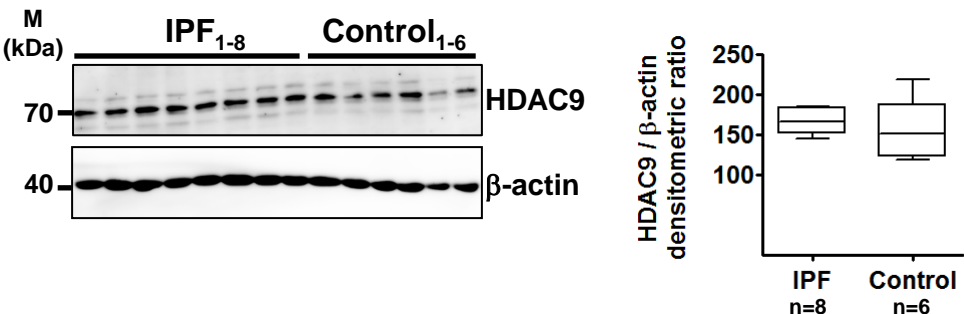
(F, G) Representative immunoblots and quantitative immunoblot analysis of human fibroblasts isolated from peripheral explanted lung tissue of patients with sporadic IPF (n=8) and non-diseased control-lungs (control, n=6) for COL1A1 (Collagen-I, F) and CD90 (G), and β-actin or GAPDH as loading control. *p<0.05, **p<0.01.

Densitometric ratios of the respective gene to GAPDH, as well as of the respective protein to β-actin or GAPDH are depicted as a box-and whisker diagram (box indicates 25th and 75th, horizontal line indicates the 50th percentile [median], and extensions above and below reflect extreme values); statistics were performed by Mann Whitney-test.



Supplementary-Figure S23: Expression analysis of histone deacetylases in primary fibroblasts isolated from idiopathic pulmonary fibrosis (IPF) - and non-diseased control-lungs (supplemental data to figure 3 of the main manuscript).

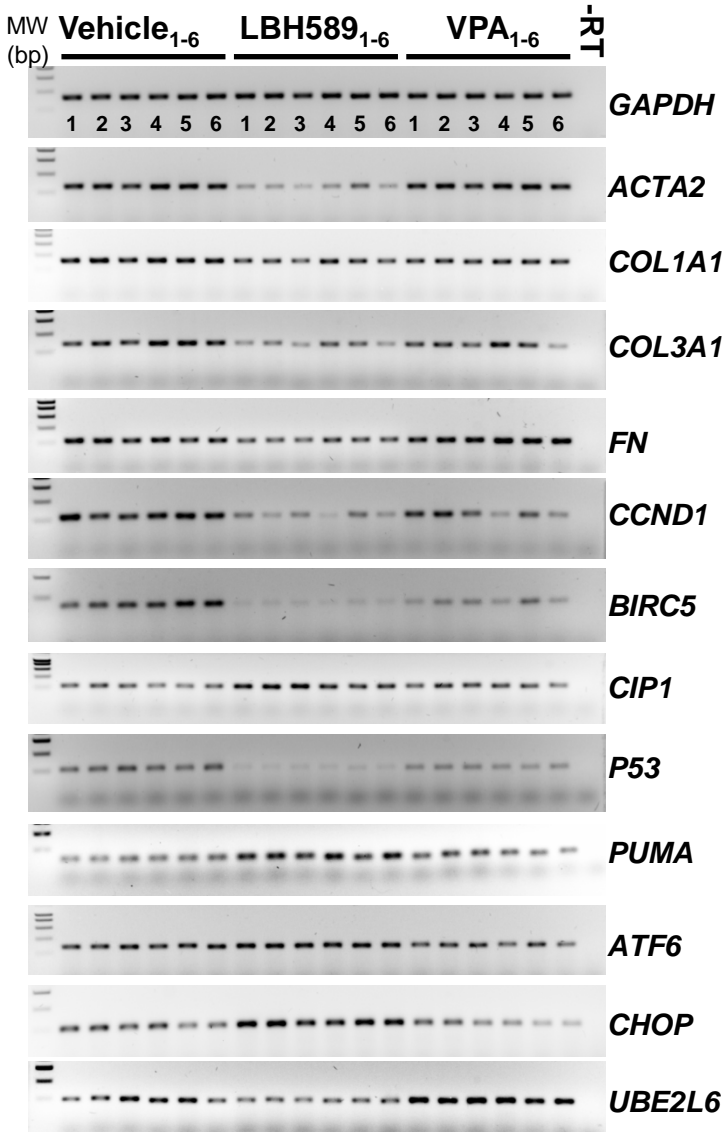
Representative agarose gels of reverse transcription-polymerase chain reactions for *HDAC2*, *HDAC3*, *HDAC4*, *HDAC5*, *HDAC7*, and *HDAC11* of human fibroblasts isolated from peripheral explanted lung tissue of patients with IPF (n=8) and non-diseased control-lungs (control, n=6). Each PCR reaction was performed with 100 ng reverse-transcribed complementary DNA, and *GAPDH* was used as reference gene. -RT control = PCR of a RNA sample without reverse transcriptase.



Supplementary-Figure S24: Protein expression analysis of histone deacetylase 9 (HDAC9) in primary fibroblasts isolated from idiopathic pulmonary fibrosis (IPF) - and non-diseased control-lungs.

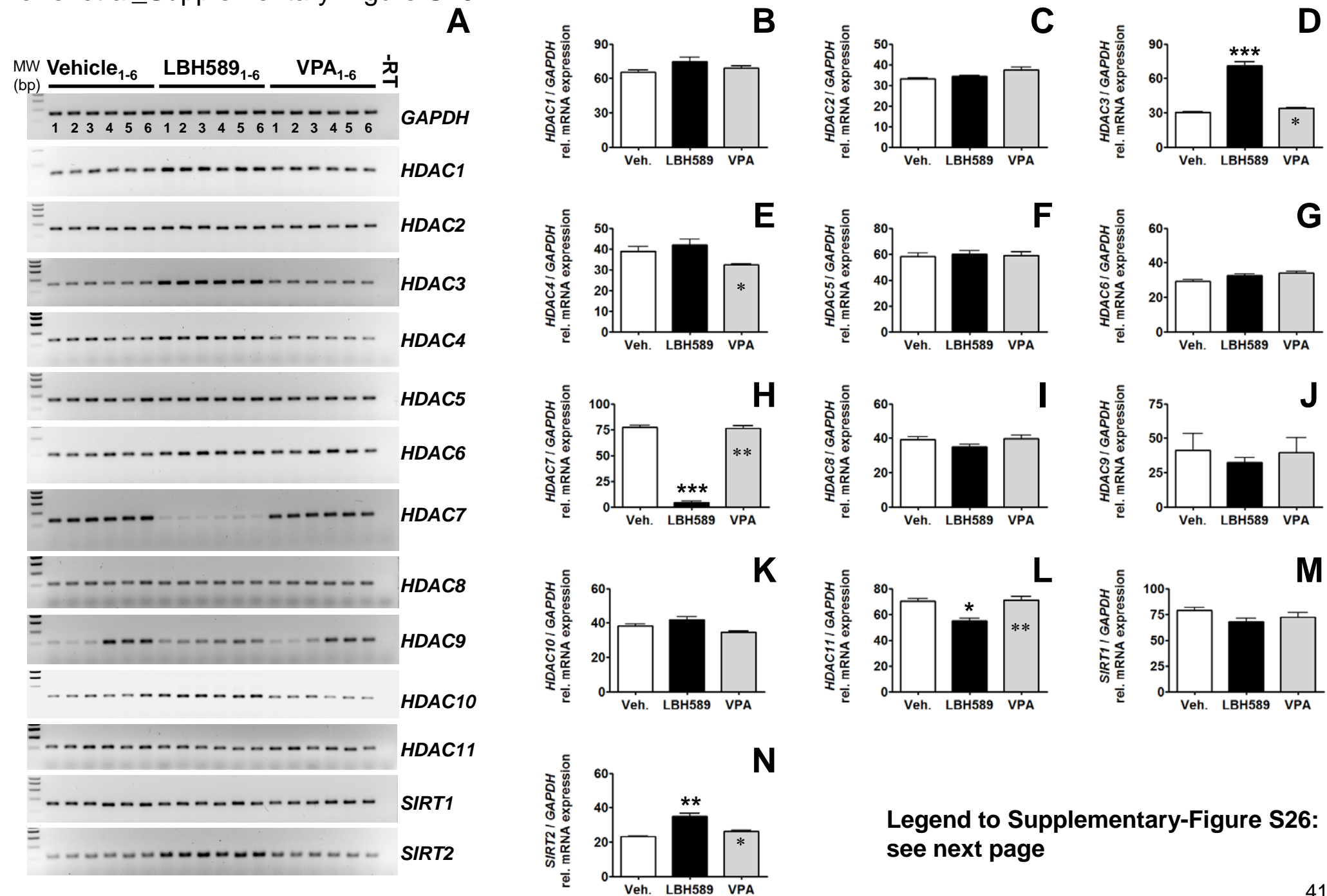
Representative immunoblot and quantitative immunoblot analysis of human fibroblasts isolated from subpleural lung tissue of patients with sporadic IPF (n=8) and non-diseased control-lungs (control, n=6) for HDAC9, by using β -actin as loading control. No significant difference in HDAC9 protein expression was observed between IPF- and control fibroblasts.

The densitometric ratio of the HDAC9 protein to β -actin is depicted as a box-and whisker diagram (*box* indicates 25th and 75th, *horizontal line* indicates the 50th percentile [median], and extensions above and below reflect extreme values).



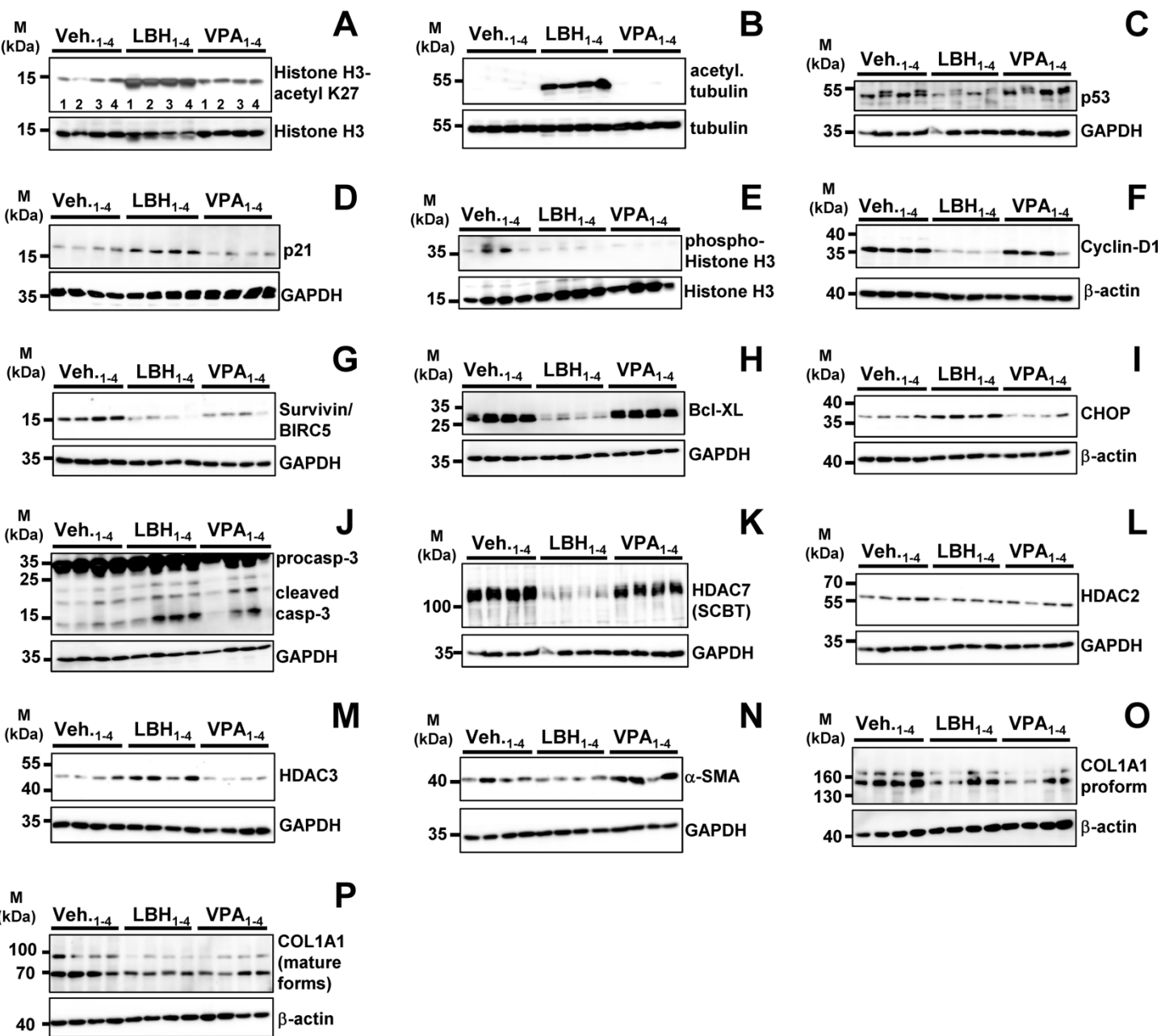
Supplementary-Figure S25: Cellular signalling in primary IPF-fibroblasts in response to treatment with panobinostat or valproic acid (supplemental data to figure 4 of the main manuscript).

Primary IPF-fibroblasts (n=6) were incubated for 30h with vehicle (0.03% DMSO, 0.1% ethanol), panobinostat (LBH589, 85 nmol) or valproic acid (VPA, 1.5 mM). The effects of vehicle - and histone deacetylase inhibitor treatments were analyzed by semiquantitative reverse transcription-polymerase chain reaction (RT-PCR) for indicated genes, and is depicted by representative agarose gels of RT-PCR products for *ACTA2*, *COL1A1*, *COL3A1*, *FN*, *CCND1*, *BIRC5*, *CIP1*, *P53*, *PUMA*, *ATF6*, *CHOP* and *UBE2L6*. Each PCR reaction was performed with 100 ng reverse-transcribed complementary DNA, and *GAPDH* was used as reference gene. -RT control = PCR of a RNA sample without reverse transcriptase.



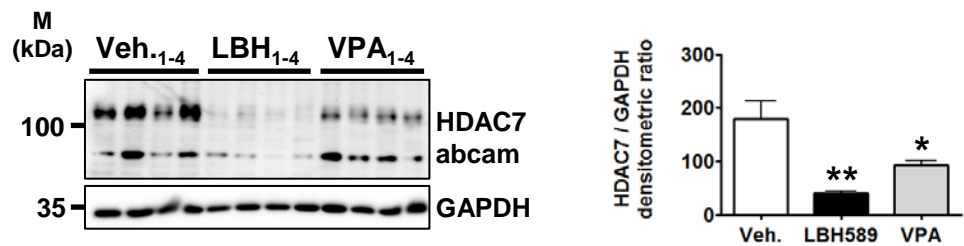
Legend to Supplementary-Figure S26: Effects of histone deacetylase inhibitor treatment on histone deacetylase gene expression in primary IPF-fibroblasts.

Primary IPF-fibroblasts (n=6) were incubated for 30h with vehicle (0.03% DMSO, 0.1% ethanol), panobinostat (LBH589, 85 nmol) or valproic acid (VPA, 1.5 mM). Gene expression of histone deacetylases (HDAC) was analyzed by semiquantitative reverse transcription-polymerase chain reaction (RT-PCR), and is depicted by representative agarose gels (**A**) and densitometric quantification of RT-PCR products for *HDAC1* (**B**), *HDAC2* (**C**), *HDAC3* (**D**), *HDAC4* (**E**), *HDAC5* (**F**), *HDAC6* (**G**), *HDAC7* (**H**), *HDAC8* (**I**), *HDAC9* (**J**), *HDAC10* (**K**), *HDAC11* (**L**), *SIRT1* (**M**), and *SIRT2* (**N**). Each PCR reaction was performed with 100 ng reverse-transcribed complementary DNA, and *GAPDH* was used as reference gene. Data are presented as mean \pm SEM of the individual values of different treatments. -RT control = PCR of a RNA sample without reverse transcriptase. *p<0.05, **p<0.01, ***p<0.001, LBH589 vs. vehicle; *p<0.05, **p<0.01 VPA vs. LBH589; by Dunn's multiple comparison test.



Supplementary-Figure S27: Analysis of acetylation status, apoptotic signalling, and profibrotic protein expression in primary IPF-fibroblasts in response to treatment with panobinostat or valproic acid (supplemental data to figure 5 of the main manuscript).

Primary IPF-fibroblasts (n=4) were incubated for 30h with vehicle (0.03% DMSO, 0.1% ethanole), panobinostat (LBH589, 85 nmol) or valproic acid (VPA, 1.5 mM). Status of acetylation, apoptosis, HDAC protein expression, and profibrotic protein expression was analyzed by quantitative immunoblotting. In dependency of research target, histone H3, GAPDH, β -actin, or tubulin served as loading control. (A) Histone H3-acetyl K27, (B) acetylated tubulin, (C) p53, (D) p21, (E) phospho-histone H3, (F) Cyclin D1, (G) Survivin, (H) Bcl-XI, (I) CHOP, (J) caspase-3, (K) HDAC7 (antibody from Santa Cruz B. I.), (L) HDAC2, (M) HDAC3, (N) α -SMA, (O) COL1A1 (pro-form), and (P) COL1A1 (mature form).



Supplementary-Figure S28: Analysis of HDAC7-protein expression in primary IPF-fibroblasts in response to treatment with panobinostat or valproic acid by immunoblotting with use of a specific antibody directed against human HDAC7 from Abcam (ab137366).

Primary IPF-fibroblasts (n=4) were incubated for 30h with vehicle (0.03% DMSO, 0.1% ethanole), panobinostat (LBH589, 85 nmol) or valproic acid (VPA, 1.5 mM), followed by lysis of fibroblastic cells and quantitative immunoblot-analysis for HDAC7. Data are presented as mean ± SEM of the individual values of different treatments. *p<0.05, **p<0.01, LBH589 or VPA vs. vehicle; by Dunn’s multiple comparison test.